

Segregation of the genus *Parahypoxylon* (Hypoxylaceae, Xylariales) from *Hypoxylon* by a polyphasic taxonomic approach

Marjorie Cedeño-Sánchez^{1,2*}, Esteban Charria-Girón^{1,2*}, Christopher Lambert^{1,2,3},
J. Jennifer Luangsa-ard⁴, Cony Decock⁵, Raimo Franke⁶,
Mark Brönstrup^{6,7}, Marc Stadler^{1,2}

1 Dept. Microbial Drugs, Helmholtz Centre for Infection Research, Inhoffenstrasse 7, 38124 Braunschweig, Germany **2** Institute of Microbiology, Technische Universität Braunschweig, Spielmannstraße 7, 38106 Braunschweig, Germany **3** Division of Molecular Cell Biology, Zoological Institute, Technische Universität Braunschweig, Spielmannstrasse 7, 38106 Braunschweig, Germany **4** National Center for Genetic Engineering and Biotechnology (BIOTEC), 113 Thailand Science Park, Phaholyothin Road, Klong Luang, Pathumthani 12120, Thailand **5** Mycothèque de l' Université catholique de Louvain (BCCM/MUCL), Place Croix du Sud 3, B-1348 Louvain-la-Neuve, Belgium **6** Department of Chemical Biology, Helmholtz Centre for Infection Research, Partner site Hannover/Braunschweig, Inhoffenstrasse 7, 38124 Braunschweig, Germany **7** German Center for Infection Research (DZIF), Site Hannover-Braunschweig, 38124 Braunschweig, Germany

Corresponding author: Marc Stadler (marc.stadler@helmholtz-hzi.de)

Academic editor: Andrew Miller | Received 28 November 2022 | Accepted 31 January 2023 | Published 20 February 2023

Citation: Cedeño-Sánchez M, Charria-Girón E, Lambert C, Luangsa-ard JJ, Decock C, Franke R, Brönstrup M, Stadler M (2023) Segregation of the genus *Parahypoxylon* (Hypoxylaceae, Xylariales) from *Hypoxylon* by a polyphasic taxonomic approach. MycoKeys 95: 131–162. <https://doi.org/10.3897/mycokeys.95.98125>

Abstract

During a mycological survey of the Democratic Republic of the Congo, a fungal specimen that morphologically resembled the American species *Hypoxylon papillatum* was encountered. A polyphasic approach including morphological and chemotaxonomic together with a multigene phylogenetic study (ITS, LSU, *tub2*, and *rpb2*) of *Hypoxylon* spp. and representatives of related genera revealed that this strain represents a new species of the Hypoxylaceae. However, the multi-locus phylogenetic inference indicated that the new fungus clustered with *H. papillatum* in a separate clade from the other species of *Hypoxylon*. Studies by ultrahigh performance liquid chromatography coupled to diode array detection and ion mobility tandem mass spectrometry (UHPLC-DAD-IM-MS/MS) were carried out on the stromatal extracts. In particular, the MS/MS spectra of the major stromatal metabolites of these species indicated the production of hitherto unreported azaphilone pigments with a similar core scaffold to the cohaerin-type metabolites, which are

* These authors contributed equally to this work.

exclusively found in the Hypoxylaceae. Based on these results, the new genus *Parahypoxylon* is introduced herein. Aside from *P. papillatum*, the genus also includes *P. ruwenzoriense* sp. nov., which clustered together with the type species within a basal clade of the Hypoxylaceae together with its sister genus *Durotheca*.

Keywords

Ascomycota, metabolite annotation, one new genus, one new species, phylogeny, polythetic taxonomy, Xylariales

Introduction

The genus *Hypoxylon* Bull. 1791 remains one of the largest in the Xylariales, even after a turbulent taxonomic history, during which its generic concept has changed drastically. Its early taxonomic history has been reviewed in great detail by Ju and Rogers (1996). Therefore, we largely refer to this monograph for the taxonomic treatments that occurred in the 19th and early 20th century.

The first world monograph of *Hypoxylon* by Miller (1961) was mainly based on stromatal morphology and ascus micromorphology. He recognized four sections (*Hypoxylon*, *Annulata*, *Appianata* and *Papillata*, the latter of which was further subdivided into two subsections, *Papillata* and *Primocinerea*). Ju and Rogers (1996) then restricted *Hypoxylon* to sections *Hypoxylon* and *Annulata*, and included several species of section *Papillata* in their emended section *Hypoxylon*. The main criteria for this taxonomic change were the presence of stromatal pigments and a nodulisporium-like anamorph. Many of the species in sections *Appianata* and *Papillata* sensu Miller (1961) do not show the latter mentioned features and were accommodated in other genera (e.g., *Biscogniauxia*, *Nemania*, *Whalleya*), which were later transferred to different families (Wendt et al. 2018). For their current classification, we refer to Hyde et al. (2020).

With the advent of molecular phylogenetic studies, and chemotaxonomy as an additional tool, the taxonomic concepts of *Hypoxylon* and other stromatic genera of the Xylariales have been further refined. The holomorphic concepts developed by Ju and Rogers, as well as other mycologists who put more emphasis on the anamorphic characters than on stromatal and ascospore morphology, have largely been confirmed. Hsieh et al. (2005) used protein-coding genes of a large number of representative taxa to resolve the phylogeny of *Hypoxylon* s. lat., which resulted in the recognition of the genus *Annulohypoxylon*. The composition of the latter genus was then equivalent to that of sect. *Annulata* sensu Ju and Rogers (1996). Notably, a parallel approach to establish a phylogeny based on ITS nrDNA sequences resulted in a very low resolution of the hypoxylid taxa (Triebel et al. 2005). Later studies revealed that a multi locus phylogeny involving both protein-coding genes and rDNA are suitable to achieve a sufficient phylogenetic resolution within *Hypoxylon* and its allies (Kuhnert et al. 2014b, 2015, 2017a; Sir et al. 2015) in scope of a polythetic concept. Concurrent chemotaxonomic studies have aided in establishing correlations between the genotypes and the phenotypes of these pyrenomycetes. Their stromatal pigments, as well as certain secondary metabolites of their mycelial cultures, turned out to be informative for

taxonomic segregation at the species or even genus level (cf. Helaly et al. 2018; Becker and Stadler 2021).

Based on the above accomplishments, Wendt et al. (2018) proposed a rearrangement of the families of the stromatic Xylariales, as well as the further segregation of genera from the mainstream of *Hypoxyylon*. The Hypoxylaceae were resurrected to accommodate *Hypoxyylon* and its closely related allies, and the Xylariaceae were restricted to the genera with geniculosporium-like anamorphs, which had already been recognized as phylogenetically distinct in earlier studies (e.g., Hsieh et al. 2010). *Annulohypoxyylon* was further subdivided and largely restricted to those species that have ostiolar rings and do not produce cohaerin-type azaphilones. The genus *Jackrogersella* was erected to accommodate those species of *Annulohypoxyylon* sensu Hsieh et al. (2005) that produce the aforementioned compounds and have papillate ostioles without rings. In addition, the genus *Pyrenopolyporus* was erected for species of *Hypoxyylon* sensu Ju and Rogers (1996) that have massive stromata, long tubular perithecia, contain naphthopyrones in their stromata and (where this is known) produce a characteristic virgariella-like anamorph. A follow-up study by Lambert et al. (2019) provided evidence that the species of the *H. monticulosum* complex differ from *Hypoxyylon* by the production of antifungal sporothriolides in culture. In addition, these fungi also lack the typical stromatal pigments of *Hypoxyylon* (Fig. 1) and appear in a basal clade in the molecular phylogeny. The genus *Hypomontagnella* was therefore introduced to accommodate them.

The genus *Hypoxyylon* in the current sense still appears heterogeneous and paraphyletic in the recently established phylogenies, also because its type species, *H. fragiforme* clustered in a relatively small clade comprising only a few species such as *H. howeanum*, *H. ticingense* and *H. rickii* (Wendt et al. 2018; Lambert et al. 2021). The latter species have in common that their stromatal pigments are of the mitorubrin type.

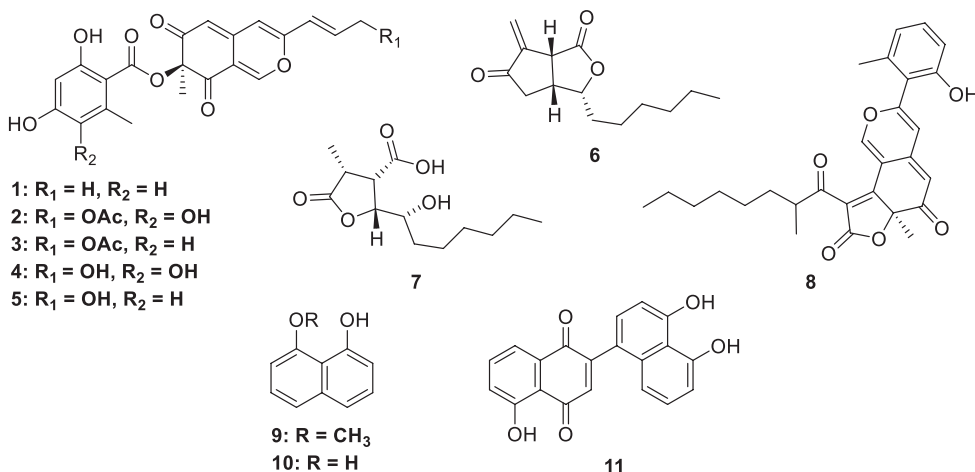


Figure 1. Characteristic stromatal pigments and other secondary metabolites of *Hypoxyylon* species. (+)-mitorubrin (**1**); (+)-6''-hydroxymitorubrinol acetate (**2**); (+)-mitorubrinol acetate (**3**); (+)-6''-hydroxymitorubrinol (**4**); (+)-mitorubrinol (**5**); sporothriolide (**6**); dihydroisoporothrone acid (**7**); cohaerin E (**8**); 8-methoxy naphthalene (**9**); 1,8-naphthol (**10**); hypoxylone (**11**).

Another species that was retained in *Hypoxylon*, even though the DNA sequences of the only available strain formed an aberrant clade in the phylogeny by Wendt et al. (2018) is *H. papillatum* Ellis & Everh. This species is characterized by effused-pulvinate stromata featuring long tubular perithecia. Therefore, its stromata somewhat resemble those of *Pyrenopolioporus* and certain *Daldinia* species such as *D. placentiformis* that do not have internal concentric zones. Ju and Rogers (1996) have studied the type material and concluded that the syntypes they studied from BPI and NY (i.e., the specimens listed in the protologue by Ellis and Everhart (see Smith 1893) did not all correspond to the same taxon. They identified some of the specimens as *Hypoxylon placentiforme* (now: *Daldinia placentiformis*), which was confirmed by Stadler et al. (2014) in the *Daldinia* world monograph, and selected a lectotype from Ohio (Commons No. 2160) which showed a characteristic morphology and could easily be distinguished from the former taxon. They also listed several other specimens from North America and Trinidad that showed the same characteristics.

Rogers (1985) cultured this fungus and provided a detailed description of its nodulisporium-like anamorph and culture. The corresponding specimen was collected by him in West Virginia, USA, and could have served as epitype. The culture is deposited in ATCC and showed the typical characteristics of *H. papillatum* sensu Rogers (1985) and was included in the phylogeny by Wendt et al. (2018) as a representative of this taxon. However, it showed an aberrant phylogenetic position in a clade that appeared basal to the others in which the DNA sequences of *Hypoxylon* species were located. We have come across a very similar fungus that was collected in Central Africa and have studied it, along with several extant type and authentic specimens for comparison. The results of this study, which also relies on state-of-the art metabolomics, are reported herein.

Materials and methods

Sample sources

All scientific names of fungi are given without authorities or publication details, according to Index Fungorum (<http://www.indexfungorum.org>). Type and reference specimens were provided by Washington State University herbarium (**WSP**), U.S. National Fungus Collections (**BPI**) and the New York Botanical Garden (**NY**), USA. Fungal cultures were provided from the Belgian Coordinated Collections of Microorganisms (**MUCL**), Belgium and the Westerdijk Fungal Biodiversity Institute (**CBS**), The Netherlands.

Morphological characterization

The microscopic characteristics of the teleomorph were carried out as described by Pourmoghaddam et al. (2020). To observe the macro-morphology of the cultures, the strains were grown on Difco Oatmeal Agar (**OA**), 2% Malt Extract Agar (**MEA**) and Yeast Malt agar (**YM** agar; malt extract 10 g/L, yeast extract 4 g/L, D-glucose 4 g/L, agar 20 g/L, pH 6.3 before autoclaving) and the cultures checked at 15 days after inoculation. Pigment colors were determined following the color-codes by Rayner (1970).

DNA extraction, PCR and sequencing

The DNA was extracted from pure cultures grown on plates with YM agar. Small amounts of mycelia were harvested after five days of growth and transferred to a 1.5 ml homogenization tube filled with six to eight Precellys Ceramic beads (1.4 mm, Bertin Technologies, Montigny-le-Bretonneux, France).

DNA extraction was performed using the commercially available Fungal gDNA Miniprep Kit EZ-10 spin column (NBS Biologicals, Cambridgeshire, UK) following the manufacturer's instructions. The *tub2* (partial β-tubulin) gene region was amplified using the primers T1 and T22 (O'Donnell and Cigelnik 1997); ITS (nuc rDNA internal transcribed spacer) region using the primers ITS4 and ITS5 (White et al. 1990); LSU (Large subunit nuc 28S rDNA) using LR0R and LR7 (Vilgalys and Hester 1990) and *rpb2* (partial second largest subunit of the DNA-directed RNA polymerase II) using fRPB2-5F and fRPB2-7cR (Liu et al. 1999).

PCR reactions were performed by mixing template gDNA (2–3 µL), 12.5 µL JumpStart Taq Ready Mix (Sigma Aldrich, Deisenhofen, Germany), 0.5 µL of both forward and reverse primers (10 mM) and 8.5 to 9.5 µl of sterile filtered and sterilized water to a final volume of 25 µL. Amplification was achieved using a Mastercycler nexus Gradient (Eppendorf, Hamburg, Germany). Thermocycling for ITS commenced with an initial denaturation at 94 °C for 5 min followed by 34 cycles of denaturation (30 s at 94 °C), annealing (30 s at 52 °C), and elongation (1 min at 72 °C). The program concluded with a 10 min lasting elongation at 72 °C and reaction tubes were stored at 4 °C until further use. In the case of the other loci, the following steps were modified: LSU denaturation (1 min at 94 °C), annealing (1 min at 52 °C), and elongation (2 min at 72 °C); For *tub2* the cycle repetitions were raised to 38, annealing (30 s at 47 °C) and elongation (2 min 30 s at 72 °C); for *rpb2*, the cycle repetitions were raised to 38, annealing (1 min at 54 °C) and elongation (1 min 30 s at 72 °C).

Molecular phylogenetic analyses

Sequences were analyzed and processed in Geneious 7.1.9 (Kearse et al. 2012). The generated sequence data were complemented by available sequence data from GenBank and the data sets for each genetic marker were aligned using MAFFT online (<http://mafft.cbrc.jp/alignment/server/>, Katoh et al. 2019), and manually curated in MEGA 11 (Tamura et al. 2021). A maximum-likelihood phylogenetic tree was constructed using IQ-TREE v. 2.1.3 [-b 1000 -abayes -m MFP -nt AUTO] (Minh et al. 2020). The selection of the appropriate nucleotide exchange model was selected by ModelFinder (Chernomor et al. 2016; Kalyaanamoorthy et al. 2017) based on Bayesian inference criterion. Branch support was calculated with non-parametric bootstrap (Felsenstein 1985 and approximate Bayes test (Anisimova et al. 2011). The total 1000 bootstrap replicates were mapped onto the ML tree with the best (highest) ML score. Single locus trees were calculated following the identical methodology and checked for congruence with the multigene phylogenetic tree.

A second phylogenetic inference was carried out following a Bayesian approach using MrBayes 3.2.7a (Ronquist et al. 2012) with algorithm options set to the ones

reported by Matio Kemkuignou et al. (2022). The data matrix was subjected to PartitionFinder2 (Lanfear et al. 2016) as implemented in the program package phylosuite v. 1.2.2 (Zhang et al. 2020) with settings set to an un-linked determination of the best-fitting nucleotide substitution models following Bayesian information criterion (BIC) for the different partitions, restricted to the ones available in MrBayes. Posterior probabilities (PP) above 95% were regarded as significant. To determine the congruence of the topologies of ML and Bayes, an approximate unbiased (AU) topology test was carried out in IQ-TREE [iqtree -s example.phy -z example.treels -n 0 -zb 10000 -zw -au](Shimodaira 2022). All sequences used for the phylogeny are listed in Table 1.

UHPLC profiling and dereplication

The secondary metabolites were extracted using a small piece of the stromata (approx. 1 mm³). Each piece was placed in 1.5 ml reaction tubes, covered with 1000 µl of methanol and placed for 30 min at 40 °C in an ultrasonic bath. The tubes were centrifuged at 14 000 rpm for 10 min. The methanol extract was separated from the remaining stromata, which was extracted again under the same procedure. Finally, both organic phases were combined and dried under nitrogen. Each sample was analyzed at a concentration of 450 µg/mL on an ultrahigh performance liquid chromatography system (Dionex Ultimate3000RS, Thermo Scientific, Dreieich, Germany), using a C18 column (Kinetex 1.7 µm, 2.1 × 150 mm, 100 Å; Phenomenex, Aschaffenburg, Germany) with a sample injection volume of 2 µL. The mobile phase consisted of A (H₂O + 0.1% formic acid) and B (ACN + 0.1% formic acid) with a constant flow rate of 0.3 mL/min. The gradient began with 1% B for 0.5 min, increasing to 5% B in 1 min, then to 100% B in 19 min and holding at 100% B for 5 min. The temperature of the column was kept at 40 °C and UV-Vis data were recorded with a DAD at 190–600 nm.

MS spectra were collected using a trapped ion mobility quadrupole time-of-flight mass spectrometer (timsTOF Pro, Bruker Daltonics, Bremen, Germany) with the following parameters: tims ramp time 100 ms, spectra rate 9.52 Hz, PASEF on, cycle time 320 ms, MS/MS scans 2, scan range (*m/z*, 100–1800 Da; 1/k₀, 0.55–2.0 V·s/cm²). For the stromatal extracts and the standards ESI mass spectra were acquired in positive ion mode. Raw data were pre-processed with MetaboScape 2022 (Bruker Daltonics, Bremen, Germany) in the retention time range of 0.5 to 25 min. The obtained features were dereplicated against our in-house database comprising MS/MS spectra of standards from characteristic secondary metabolites of hypoxylaceous species (e.g. azaphilones, asterriquinones, binaphthalenes, cytochalasins, macrolides and sesquiterpenoids) in MetaboScape. A molecular network was created with the Feature-Based Molecular Networking (FBMN) (Nothias et al. 2020) and the Spec2Vec (Huber et al. 2021) workflows on the GNPS platform (Wang et al. 2016) using the pre-processed feature table from MetaboScape. Fragmentation ions resulting from the MS/MS spectra of cohaerin E, cohaerin H, and minutellin A were assigned using CFM-ID 4.0 web server (Wang et al. 2021) and validated with the SmartFormula 3D tool from MetaboScape. The datasets generated/analyzed for this study are included in Suppl. material 1.

Table I. Strains used in the phylogenetic analyses, including the strain IDs, GenBank accession numbers, and the references where the sequence data have been originally generated. Type specimens are labeled with T (holotype), IT (isotype), PT (paratype) and ET (epitype).

Species	Strain number	GenBank Accession Number			Origin	References	
		ITS	LSU	<i>rpb2</i>	<i>mtb2</i>		
<i>Annulohypoxyylon annulatum</i>	CBS 140775	KY610418	KY624463	KX376353	USA (ET)	Kuhnert et al. (2018; ITS, LSU, <i>rpb2</i>)	
<i>Annulohypoxyylon michelianum</i>	CBS 119993	KX376320	KY610423	KY624234	Spain	Kuhnert et al. (2014a; ITS, <i>tub2</i>), Wendt et al. (2018; LSU, <i>rpb2</i>)	
<i>Annulohypoxyylon truncatum</i>	CBS 140778	KY610419	KY610419	KY624277	USA (ET)	Kuhnert et al. (2014a; ITS, <i>tub2</i>), Wendt et al. (2018; ITS, LSU, <i>rpb2</i>)	
<i>Daldinia bambusicola</i>	CBS 122872	KY610385	KY610431	KY624241	Thailand (T)	Hsieh et al. (2005; <i>tub2</i>), Wendt et al. (2018; ITS, LSU, <i>rpb2</i>)	
<i>Daldinia chilida</i>	CBS 122881	KU683375	MH684273	KU684129	France (T)	URen et al. (2016; ITS, <i>tub2</i> , <i>rpb2</i>), Vu et al. (2019; LSU)	
<i>Daldinia concentrica</i>	CBS 113277	AY616683	KY610434	KY624243	Germany	Triebel et al. (2005; ITS), Kuhnert et al. (2014a; <i>tub2</i>), Wendt et al. (2018; LSU, <i>rpb2</i>)	
<i>Daldinia demitii</i>	CBS 114741	JX658477	KY610435	KY624244	KC977262	Australia (T)	Stadler et al. (2014; ITS), Kuhnert et al. (2014a; <i>tub2</i>), Wendt et al. (2018; LSU, <i>rpb2</i>)
<i>Daldinia eschscholtzii</i>	MUCL 45435	JX658484	KY610437	KY624246	KC977266	Benin	Stadler et al. (2014a; ITS), Kuhnert et al. (2014a; <i>tub2</i>), Wendt et al. (2018; LSU, <i>rpb2</i>)
<i>Daldinia perminae</i>	MUCL 49214	AM74937	KY610439	KY624248	KC977261	Austria (ET)	Bitter et al. (2008; ITS), Kuhnert et al. (2014a; <i>tub2</i>), Wendt et al. (2018; LSU, <i>rpb2</i>)
<i>Daldinia placentiformis</i>	MUCL 47603	AM74921	KY610440	KY624249	KC977278	Mexico	Stadler et al. (2014a; ITS), Kuhnert et al. (2014a; <i>tub2</i>), Wendt et al. (2018; LSU, <i>rpb2</i>)
<i>Daldinia vernicosa</i>	CBS 119316	KY610395	KY610442	KY624252	KC977260	Germany (ET)	Kuhnert et al. (2014a; <i>tub2</i>), Wendt et al. (2018; ITS, LSU, <i>rpb2</i>)
<i>Dumetella rogersii</i>	YMJ 92031201	EF026127	JX507794	EF025612	Taiwan	Ju et al. (2007) as <i>Theisia rogersii</i>	
<i>Dumetella conoides</i>	YMJ 90071615	EF026128	JX507793	EF025613	Taiwan (T)	Ju et al. (2003) as <i>Theisia rogersii</i>	
<i>Dumetella crateriformis</i>	GMBCo205	MH645426	MH645425	MH049441	China (T)	de Long et al. (2019)	
<i>Dumetella guizhouensis</i>	GMBCo0065	MH645423	MH645421	MH645422	MH049439	China (T)	de Long et al. (2019)
<i>Dumetella rogersii</i>	GMBCo204	MH645433	MH645434	MH645435	MH049449	China	de Long et al. (2019)
<i>Gymphostroma platystomum</i>	CBS 270.87	JX658335	DQ836906	KY624296	HG934108	France (T)	Zhang et al. (2006; LSU), Stadler et al. (2014; ITS), Koukol et al. (2015; <i>tub2</i>), Wendt et al. (2018; <i>rpb2</i>)
<i>Hypomortagella barbarensis</i>	STMA 14081	MK131720	MK131718	MK135891	MK135893	Argentina (T)	Lambert et al. (2019)
<i>Hypomortagella monticulosa</i>	MUCL 54604	KY610404	KY610487	KY624305	KX271273	French Guiana	Wendt et al. (2018)
<i>Hypomortagella submonticulosa</i>	CBS 115280	KC968923	KY610457	KY624226	KC977267	France	Kuhnert et al. (2014a; ITS, <i>tub2</i>), Wendt et al. (2018; LSU, <i>rpb2</i>)
<i>Hypoxyylon addis</i>	MUCL 52797	KC968931	ON954141	OP251037	KC977287	Ethiopia (T)	Kuhnert et al. (2014a; ITS, <i>tub2</i>), This study
<i>Hypoxyylon ariense</i>	MUM 1940	MN053021	ON954142	OP251028	MN066636	Portugal (T)	Vicente et al. (2021; ITS, <i>tub2</i>), This study
<i>Hypoxyylon burrunense</i>	UCH9545	MN056428	ON954143	MK98142	Panama (T)	Cedeno-Sánchez et al. (2020; ITS, <i>tub2</i>); This study	
<i>Hypoxyylon carnaense</i>	MUCL 47224	ON792387	ON954140	OP251029	ON813073	Spain, Canary Islands (PT)	This study, (Species described by Stadler et al. 2008)
<i>Hypoxyylon carneum</i>	MUCL 54177	KY610400	KY610480	KY624297	KX271270	France	Wendt et al. (2018)
<i>Hypoxyylon crenicola</i>	CBS 119009	KC968908	KY610444	KY624254	KC977263	France	Kuhnert et al. (2014a; ITS, <i>tub2</i>), Wendt et al. (2018; LSU, <i>rpb2</i>)
<i>Hypoxyylon chinotomum</i>	STMA 14060	KU604563	ON954144	OP251030	ON813072	Argentina	Sir et al. (2016; ITS); This study

Species	Strain number	GenBank Accession Number			Origin	References	
		ITS	LSU	rpb2	mb2		
<i>Hypoiodylon chrysoidesporum</i>	FCATA32710	OL467294	OL615106	OL584222	OL584229	China (T)	Ma et al. (2022)
<i>Hypoiodylon erioccephalum</i>	CBS 110904	KC968907	KY610445	KY624255	KC977268	France	Kuhnert et al. (2014a; ITS, <i>tub2</i>), Wendt et al. (2018; LSU, <i>rpb2</i>)
<i>Hypoiodylon cyclocladidomycetidis</i>	FCATA32714	OL467298	OL615108	OL584225	OL584232	China (T)	Ma et al. (2022)
<i>Hypoiodylon erythrostroma</i>	MUCL 533759	KC968910	ON954154	OP251031	KC977296	Martinique	Kuhnert et al. (2014a; ITS2, TUB), This study
<i>Hypoiodylon eutaiatium</i>	MUCL 577720	MW367851	MW373852	MW373861		Iran (T)	Lambert et al. (2021)
<i>Hypoiodylon felandii</i>	MUCL 54792	KF234421	KY610481	KY624298	KF309080	French Guiana	Kuhnert et al. (2014a; ITS, <i>tub2</i>), Wendt et al. (2018; LSU, <i>rpb2</i>)
<i>Hypoiodylon ferrugineum</i>	CBS 141259	KX09079	KM186295	MK887342	KX271282	Austria	Friebes and Wendelin (2016)
<i>Hypoiodylon fragiforme</i>	MUCL 51264	KC477229	KM186295			Germany (ET)	Städler et al. (2013; ITS), Darangama et al. (2015; LSU, <i>rpb2</i>), Wendt et al. (2018; <i>tub2</i>)
<i>Hypoiodylon fascoides</i>	MUCL 52670	ON792789	ON954145	OP251038	ON813076	France (T)	This study. (Species described by Fourrier et al. 2010a)
<i>Hypoiodylon ficium</i>	CBS 113049	KY610401	KY610482	KY624299	KX271271	Germany (ET)	Wendt et al. (2018)
<i>Hypoiodylon gibricinense</i>	MUCL 52698	KC968930	ON954146	OP251026	ON813074	France (T)	Kuhnert et al. (2014a; ITS), This study
<i>Hypoiodylon griseobrunneum</i>	CBS 33173	KY610402	KY610483	KY624300	KC977303	India (T)	Kuhnert et al. (2014a; <i>tub2</i>), Wendt et al. (2018; ITS, LSU, <i>rpb2</i>)
<i>Hypoiodylon guadalupense</i>	MUCL 577726	MT214997	MT214992	MT212235	MT212239	Iran (T)	Pournoghdaddam et al. (2020)
<i>Hypoiodylon haematostruma</i>	MUCL 53301	KC968911	KY610484	KY624301	KC977291	Martinique (ET)	Wendt et al. (2018; LSU, <i>rpb2</i>), Kuhnert et al. (2014a; ITS, <i>tub2</i>)
<i>Hypoiodylon hainanense</i>	FCATA32712	OL467296	OL616132	OL584224	OL584231	China (T)	Ma et al. (2022)
<i>Hypoiodylon himalaeum</i>	ATCC 36255	MK287537	MK287537	MK287562	MK287575	USA (T)	Sir et al. (2019)
<i>Hypoiodylon howeanum</i>	MUCL 3621	AM749928	KY610448	KY624258	KC977277	Germany	Bitzer et al. (2008; ITS), Kuhnert et al. (2014a; <i>tub2</i>), Wendt et al. (2018; LSU, <i>rpb2</i>)
<i>Hypoiodylon hypomitum</i>	MUCL 51845	KY610403	KY610449	KY624302	KX271249	Guadeloupe	Wendt et al. (2018)
<i>Hypoiodylon invadens</i>	MUCL 51475	M1809133	M1809133	MT813037	MT813038	France (T)	Becker et al. (2020)
<i>Hypoiodylon inveniens</i>	CBS 118183	KC968925	KY610450	KY624259	KC977270	Malaysia	Kuhnert et al. (2014a; ITS, <i>tub2</i>), Wendt et al. (2018; LSU, <i>rpb2</i>)
<i>Hypoiodylon isabellinum</i>	MUCL 53308	KC968935	ON954155	OP251032	KC977295	Martinique (T)	Kuhnert et al. (2014a; ITS, <i>tub2</i>), This study
<i>Hypoiodylon lachilli</i>	MUCL 52796	JX658325	ON954147	OP251027	ON813075	France	Städler et al. (2014; ITS, <i>tub2</i>), Wendt et al. (2018; ITS, <i>rpb2</i>)
<i>Hypoiodylon lateripigmentatum</i>	MUCL 53304	KC968933	KY610486	KY624304	KC977290	Martinique (T)	Kuhnert et al. (2014a; ITS, <i>tub2</i>), This study
<i>Hypoiodylon lechattii</i>	MUCL 54609	KP923407	ON954148	OP251033	KP923405	French Guiana	Kuhnert et al. (2014a; ITS, <i>tub2</i>), Wendt et al. (2018; LSU, <i>rpb2</i>)
<i>Hypoiodylon lenormandii</i>	CBS 119003	KC968943	KY610452	KY624261	KC977273	Ecuador	Kuhnert et al. (2014a; ITS, <i>tub2</i>), Wendt et al. (2018; LSU, <i>rpb2</i>)
<i>Hypoiodylon lienhuaense</i>	MFLUCC 14-1231	KU604558	MK287550	MK287553	KU159522	Thailand	Sir et al. (2016; ITS, <i>tub2</i>), Sir et al. (2019; LSU, <i>rpb2</i>)
<i>Hypoiodylon linddipigmentum</i>	STIMA14045	ON792788	ON954149		ON813077	Argentina	This study
<i>Hypoiodylon linddipigmentum</i>	BCRG-34077	JN97933			AY951735	Mexico (T)	Hiich et al. (2005)
<i>Hypoiodylon macrocarpum</i>	CBS119012	ON792785	ON954151	OP251034	ON813071	Germany	This study
<i>Hypoiodylon minkai</i>	MUCL 53315	KC968912	ON954153	OP251035	KC977294	Martinique	Kuhnert et al. (2014a; ITS, <i>tub2</i>), This study
<i>Hypoiodylon muscicarum</i>	MUCL 53765	KC968926	KY610488	KY624306	KC977280	Guadeloupe	Kuhnert et al. (2014a; ITS, <i>tub2</i>), Wendt et al. (2018; LSU, <i>rpb2</i>)
<i>Hypoiodylon ochraceum</i>	MUCL 54625	KC968937		KY624271	KC977300	Martinique (ET)	Kuhnert et al. (2014a; ITS, <i>tub2</i>), Wendt et al. (2018; <i>rpb2</i>)

Species	Strain number	GenBank Accession Number			Origin	References
		ITS	LSU	rpB2		
<i>Hypoxyylon olivaceopigmentum</i>	DSM 107924	MK287530	MK287542	MK287555	MK287568	USA (T) France
<i>Hypoxyylon perforatum</i>	CBS 1151281	KY610391	KY610455	KY624224	KX271250	France
<i>Hypoxyylon pernitiae</i>	CBS 1147446	KY610405	KY610491	KY624279	KX271274	France (T)
<i>Hypoxyylon pilosum</i>	STMA 14355	KY6104142	KY610412	KY624308	KY624315	Martinique
<i>Hypoxyylon porphyreum</i>	CBS 110922	KC968921	KY610456	KY624232	KC977264	France
<i>Hypoxyylon psuoflavum</i>	DSM 112038	MW367857	MW373858	MW373867	MW373867	Germany (T)
<i>Hypoxyylon pulchellum</i>	CBS 122622	JX183075	KY610492	KY624280	JX183072	Martinique (T)
<i>Hypoxyylon rickii</i>	MUCL 53309	KC968932	KY610416	KY624281	KC977288	Martinique (ET)
<i>Hypoxyylon rubiginosum</i>	MUCL 52887	KC477232	KY610469	KY624266	KY624311	Germany (ET)
<i>Hypoxyylon sanctaei</i>	MUCL 51843	KC968916	KY610466	KY624269	KC977286	Guadeloupe (ET)
<i>Hypoxyylon spirirritatumicum</i>	MN056426	ON954150	OP251036	MK98140	Panama (T)	Panama (T)
<i>Hypoxyylon subtropicense</i>	MUCL 53752	KC968913	ON954152	KC977297	MK287561	French Guiana
<i>Hypoxyylon tenuissime</i>	DSM 107933	MK287536	MK287548	MK287574	USA (T)	USA (T)
<i>Hypoxyylon tenuissime</i>	CBS 115271	JQ009317	KY610471	KY624272	AY951757	France
<i>Hypoxyylon trigoides</i>	MUCL 54794	KF254422	KY610493	KY624282	KP305458	Sri Lanka (ET)
<i>Hypoxyylon vogesiacum</i>	CBS 115273	KC968920	KY610417	KY624283	KX271275	France
<i>Hypoxyylon unzibhanense</i>	FCATAS2708	OL467292	OL615104	OL584220	OL584227	China (T)
<i>Jackrogersella cohaerens</i>	CBS 119126	KY610396	KY610497	KY624270	KY624314	Germany (ET)
<i>Jackrogersella multiflora</i>	CBS 119016	KC477234	KY610473	KY624290	KX271262	Germany (ET)
<i>Natamodula speciosa</i>	CLM-RV86	MF380435	MF380435	MH745150	Mexico (T)	Mexico (T)
<i>Parahypoxyylon papillatum</i> comb. nov.	ATCC 58729	KC968919	KY610454	KY624223	KC977258	USA (T)
<i>Parahypoxyylon ruvenzoriense</i> sp. nov.	MUCL 51392	ON792786	ON954156	OP251039	ON813078	D. R. Congo (I)
<i>Pyrenopophyton hanteri</i>	MUCL 52673	KY610421	KY610472	KY624309	KU159550	Ivory Coast (ET)
<i>Pyrenopophyton laminosus</i>	MUCL 53305	KC968934	KY610485	KY624303	KC977292	Martinique (T)
<i>Pyrenopophyton nicaraguense</i>	CBS 117739	AM749922	KY610489	KY624307	KC977272	Burkina_Faso
<i>Rhopalostroma angolense</i>	CBS 126414	KY610420	KY610459	KY624228	KX271277	Ivory Coast
<i>Rostrohypoxylon terebratum</i>	CBS 119137	DQ631943	DQ840069	DQ631954	DQ840097	Thailand (T)
<i>Rauvencoria pseudoannulata</i>	MUCL 51394	KY610406	KY610494	KY624286	KX271278	D. R. Congo (T)
<i>Thamnomyces dendroidea</i>	CBS 123578	FN428831	KY610467	KY624232	KY624313	French Guiana (T)
<i>Xylaria arbuscula</i>	CBS 126415	KY610394	KY610463	KY624287	KX271257	Germany
<i>Xylaria hypoxylon</i>	CBS 122620	KY610407	KY610495	KY624231	KX271279	Sweden (ET)

Lambert et al. (2021)
 Bills et al. (2012; ITS, *tub2*), Wendt et al. (2018; LSU, *rpB2*)
 Kuhnert et al. (2014a; ITS, *tub2*), Wendt et al. (2018; LSU, *rpB2*)
 Kuhnert et al. (2014a; ITS, *tub2*), Wendt et al. (2018; *tub2*, LSU, *rpB2*)
 Stadler et al. (2013; ITS), Wendt et al. (2018; *tub2*, *rpB2*)
 Kuhnert et al. (2014a; ITS, *tub2*), Wendt et al. (2018; LSU, *rpB2*)
 Cedeno-Sanchez et al. (2020; ITS, *tub2*); This study
 Kuhnert et al. (2014a; ITS, *tub2*), This study
 Hsieh et al. (2005; ITS, *tub2*), Wendt et al. (2018; LSU, *rpB2*)
 Kuhnert et al. (2014a; ITS, *tub2*), Wendt et al. (2018; *tub2*), Wendt et al. (2017a; *tub2*), Wendt et al. (2018; LSU, *rpB2*)
 Ma et al. (2022)
 Wendt et al. (2018)
 Kuhnert et al. (2014a; ITS, *tub2*), Wendt et al. (2017a; *tub2*), Wendt et al. (2018; LSU, *rpB2*)
 Heredia et al. (2020)
 Kuhnert et al. (2014a; ITS, *tub2*), Wendt et al. (2018; LSU, *rpB2*)
 This study
 Kuhnert et al. (2017a; *tub2*), Wendt et al. (2018; ITS, LSU, *rpB2*)
 Kuhnert et al. (2014a; ITS, *tub2*), Wendt et al. (2018; *tub2*), Wendt et al. (2017a; *tub2*), Wendt et al. (2018; LSU, *rpB2*)
 Fournier et al. (2011; ITS), Wendt et al. (2018; *tub2*, LSU, *rpB2*)
 Wendt et al. (2018)

Results

Phylogenetic analyses

The final data matrix for the molecular phylogenetic analysis (Fig. 2) comprised 345 sequences (44 generated in this study, and complemented by sequences available from GenBank, NCBI) derived from 89 strains and four loci, namely ITS, LSU, *rpb2* and *tub2*. The final MAFFT alignments consisted of 4018 nucleotides for the ITS alignment, 3642 for the LSU alignment, 2238 for the *tub2* alignment and 4023 positions for the *rpb2* alignment. The alignment of each locus is available in the Suppl. material 1: table S3–S6. Sequences of representatives for each molecularly well-established genus of the Hypoxylaceae were included: *Annulohypoxylon* (3 strains), *Daldinia* (8 strains), *Durotheeca* (5 strains), *Hypomontagnella* (3 strains), *Hypoxylon* (58 strains), *Jackrogersella* (2 strains), *Natonodosa* (1 strain), *Pyrenopolyporus* (3 strains), as well as *Rhopalostroma*, *Rostrohypoxylon*, *Ruwenzoria*, and *Thamnomyces* (1 strain each). Three members of Xylariaceae and Graphostromataceae (*Xylaria hypoxylon*, *X. arbuscula* and *Graphostroma platystomum*) served as outgroup.

The inference of phylogenetic relationship using a Maximum-Likelihood and Bayesian approach yielded two different, incongruent topologies. An approximate unbiased (AU) topology test implemented in IQTree indicated that the tree resulting from Bayesian inference received a significantly ($p < 0.05$) lower maximum likelihood score, suggesting its rejection. Hence, we included support values of the approximate Bayes test implemented in IQTree to access posterior probability support values of the inferred phylogenetic tree. The combined rooted phylogenetic tree showed a clade consisting of the core members of the Hypoxylaceae, such as *Hypoxylon*, *Daldinia*, *Pyrenopolyporus*, *Hypomontagnella*, *Jackrogersella*, *Rostrohypoxylon*, *Thamnomyces* and *Ruwenzoria* with medium BS and high PP support (1/90), which was placed in a sister position to a clade consisting of members of *Parahypoxylon* gen. nov., and *Durotheeca* (Hypoxylaceae) at the base of the tree with strong support (1/100). The genus *Hypoxylon* could be confirmed as paraphyletic, as has been described already by Wendt et al. (2018), Lambert et al. (2019), and Becker et al. (2020). The sequences assigned to *Parahypoxylon ruwenzoriense* formed a highly supported (1/100) cluster with the sequences derived from *Parahypoxylon papillatum*. The topology of *Durotheeca* and the newly described genus *Parahypoxylon* as a basal lineage in the Hypoxylaceae are further reflected upon in the taxonomic part of this study.

Taxonomy

Lecto- and epitypification

Hypomontagnella monticulosa (Mont.) Sir, L. Wendt & C. Lamb.

Type. French Guiana, Cayenne, Leprieur, C. 1176, dead wood (PC, holotype; FH, isotype of *H. monticulosum*).

Epitype (designated here). FRANCE. French Guyana, Sinnamary, Paracou, Amazonian rain forest, bark of unknown tree, June 2012, leg J. Fournier (LIP, ex-epitype

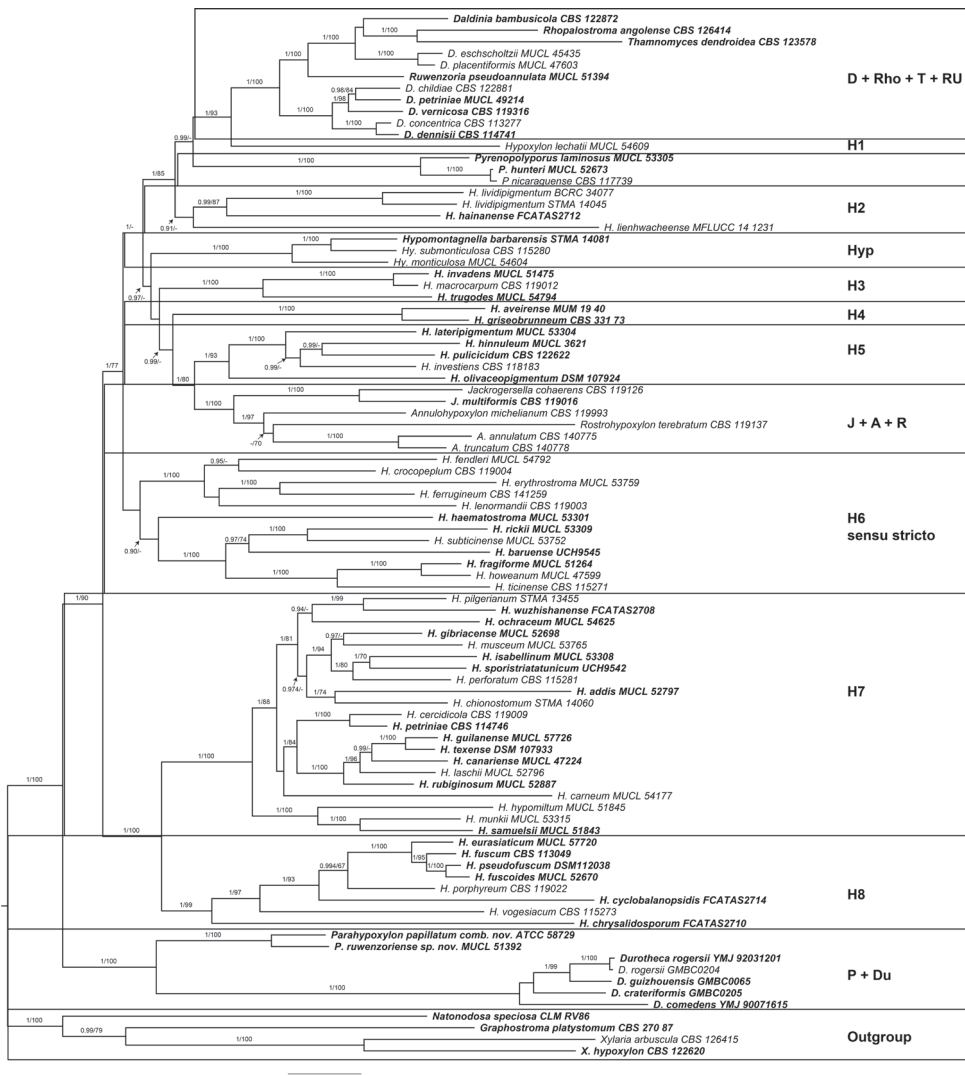


Figure 2. Inferred molecular phylogenetic maximum Likelihood ($\text{ILn} = -122825.7921$) tree of selected Hypoxylaceae, Graphostromataceae and Xylariaceae sequences. The analysis was calculated by using IQ-TREE with posterior probability support calculated from Bayesian inference methodology and support values generated from 1000 bootstrap replicates using a multigene alignment (ITS, LSU, *tub2* and *rpb2*). The tree was rooted with *Xylaria hypoxylon* CBS 122620, *X. arbuscula* CBS 126415 (Xylariaceae) and *Graphostroma platystomum* CBS 27087 (Graphostromataceae). Type material is highlighted in **bold** letters. Bayesian posterior probability scores ≥ 0.95 / Bootstrap support values ≥ 70 are indicated along branches.

culture MUCL 54604). GenBank acc. nos for DNA sequences: KY610404 and KJ810556 (ITS), KY610487 (LSU), KY624305 (*rpb2*), KX271273 (*tub2*); MT889334 (sporothriolide gene cluster published by Tian et al. 2020).

MBT no: 10010042.

Notes. The strain designated here as epitype was used by Lambert et al. (2019) and the subsequent publications on genome analysis (Stadler et al. 2020; Tian et al. 2020; Kuhnert et al. 2021; Wibberg et al. 2021). The specimen and culture are perfectly suitable, because it was collected from the same geographic area as the holotype.

***Parahypoxylon* M. Cedeño-Sánchez, E. Charria-Girón & M. Stadler, gen. nov.**

MycoBank No: 845463

Etymology. Refers to the morphological similarity to *Hypoxylon*, from which the genus is phylogenetically distinct.

Diagnosis. Differs from the genus *Durotheca* by the presence of greenish KOH-extractable pigments and by having an amyloid ascal apical apparatus. Differs from the genus *Hypoxylon* by containing yet unknown cohaerin-type azaphilones and by its basal position in the molecular phylogenetic inference using am ITS, LSU, *rpb2* and *tub2* matrix.

***Parahypoxylon papillatum* (Ellis & Everh.) M. Cedeño-Sánchez, E. Charria-Girón & M. Stadler, comb. nov.**

MycoBank No: 845462

Figs 3, 4

Hypoxylon papillatum Ellis & Everh. in Smith, Bull. Lab. Nat. Hist. Iowa State Univ. 2: 408 (1893). Syn.

Lectotype. USA. Ohio, Delaware, 21 Jul 1893, A. Commons 2160, rotten wood of *Carya* (NY [2 pks.], selected by Ju and Rogers (1996).

Epitype. USA. West Virginia, Mason Co., Bruce's Chapel, 18 Aug 1983, wood of *Acer*, J.D. Rogers (WSP 7557; ex-epitype culture ATCC 58729).

MBT no: 10011515.

Teleomorph. Stromata superficial, effused-pulvinate to plane, with inconspicuous to conspicuous perithecial mounds, up to 12.5 cm long × up to 4 cm broad × 1.8–4.0 mm thick; surface Honey (64) to Isabelline (65), Isabelline (65) to Gray Olivaceous (107), or Isabelline (65) to Olivaceous (48); blackish granules immediately beneath surface and between perithecia, with KOH-extractable pigments Isabelline (65); the tissue below the perithecial layer conspicuous, black, 1.0–2.5 mm thick. Perithecia long-tubular, 0.3–0.4 mm diam × 0.8–1.5 mm high. Ostioles umbilicate. Asci with amyloid, discoid apical apparatus, 1–2 µm high × 3.5 µm wide, stipe up 137–180 µm long × 8–10 µm broad, the spore-bearing parts 93–110 µm long, the stipes 30–80 µm long. Ascospores brown to dark brown, unicellular, ellipsoid, nearly equilateral, with broadly to narrowly rounded ends, 12.0–18.5 × 6.5–9.0 µm, with straight germ slit spore-length; perispore indehiscent in 10% KOH; episporae smooth.

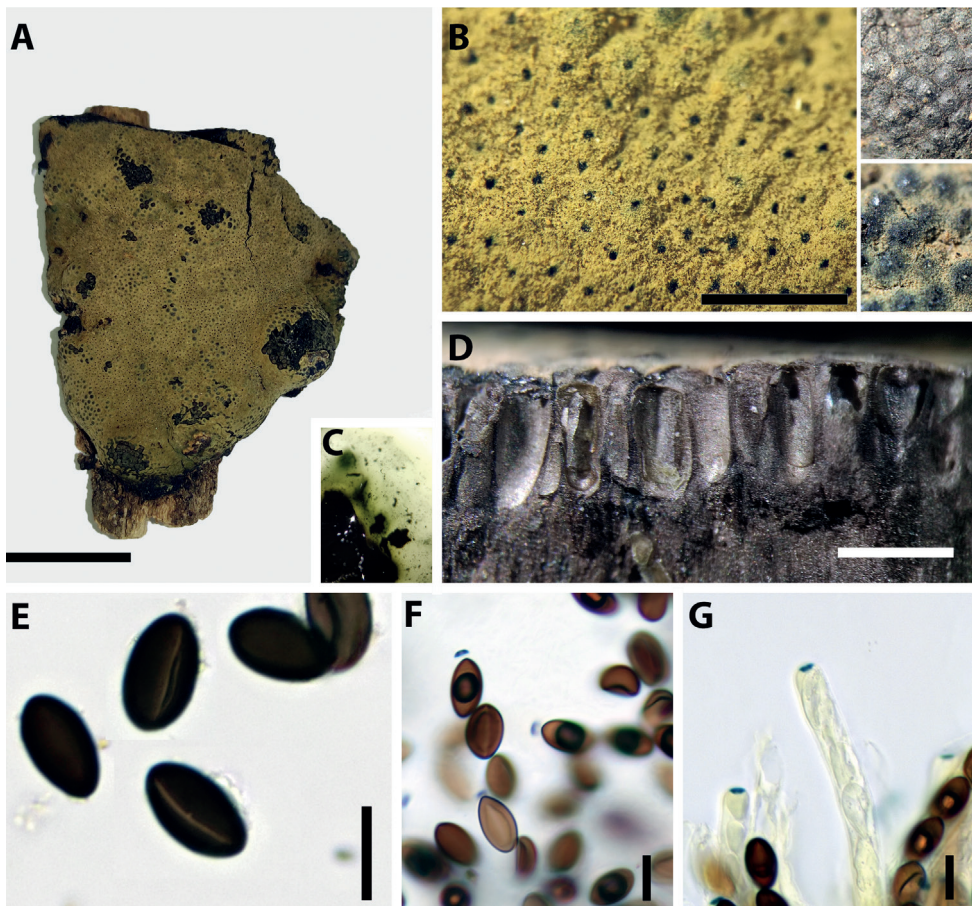


Figure 3. *Parahypoxylon papillatum* comb. nov. **A** stroma **B** ostioles **C** KOH extractable stromatal pigments **D** perithecia (cross section) **E** ascospores with straight germ slits **F** amyloid apical apparatus in a mature ascus treated with Melzer's reagent **G** amyloid apical apparatus in an immature ascus treated with Melzer's reagent. Scale bars: 1 cm (**A**); 10 µm (**E–F**); 10 µm (**G**).

Cultures and anamorph. Colonies on MEA, OA, and YM covering a 9 cm Petri plate in 2 weeks, with white, flat, mycelium, margins filamentous. Reverse at first white, becoming yellowish at the center. The anamorph has been described by Rogers (1985), but we were unable to confirm the presence of conidial structures when we studied the strain more than 30 years later.

Secondary metabolites. Stromata contain BNT and cohaerin type azaphilones according to the MS/MS analysis.

Notes. We were not only able to confirm the morphometric results of Ju and Rogers (1996) but even established that this species is characterized by a rather specific metabolite profile. This species has to our knowledge still not been reported from outside America and seems to be most frequently encountered in the Eastern USA.

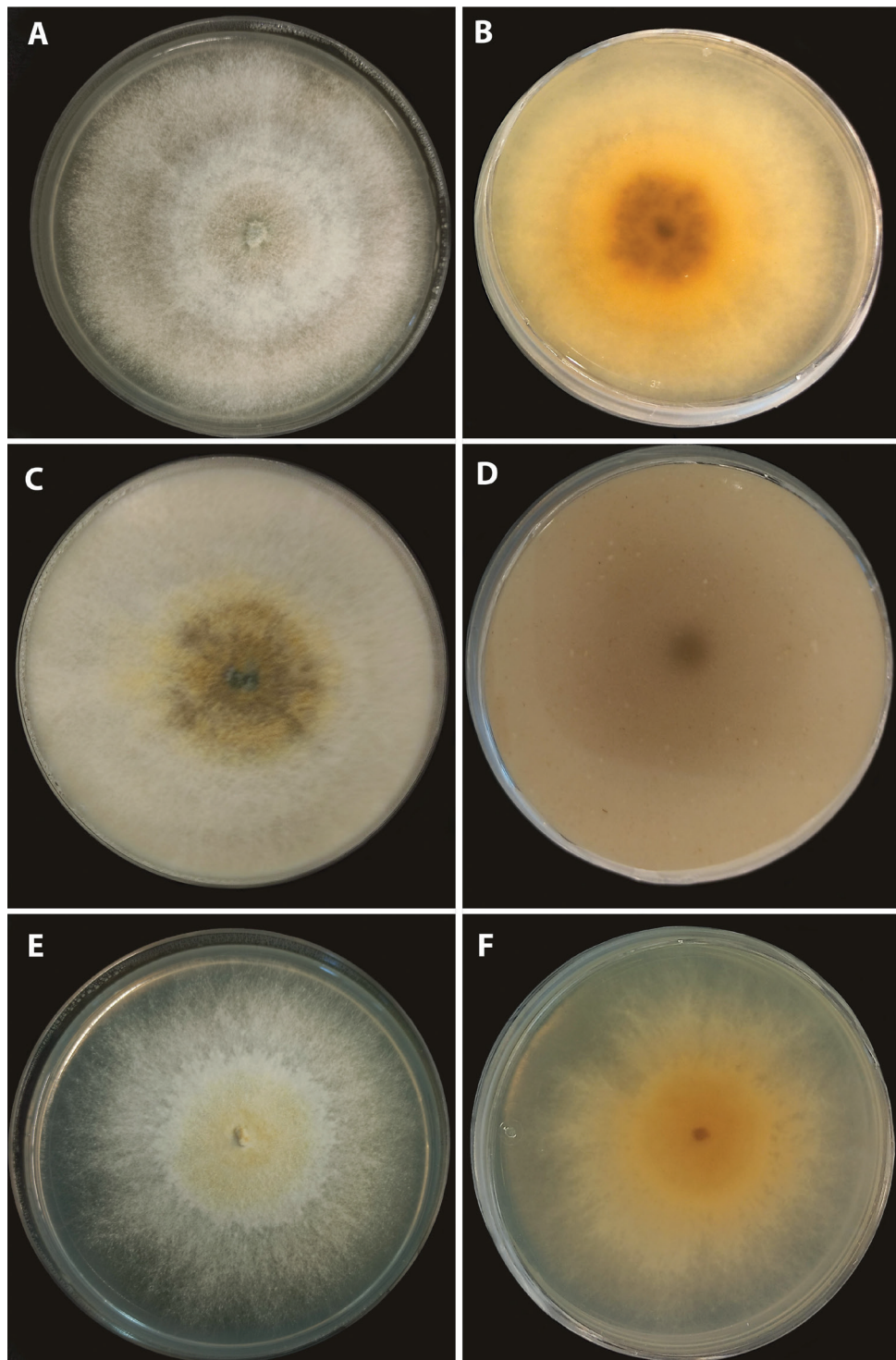


Figure 4. *Parahypoxylon papillatum* comb. nov. (ATCC 58729) Colonies after 2 weeks (**A, B**) on 2% MEA (**C, D**) on OA (**E, F**) on YM.

Further specimens examined. USA. Kansas, on decorticated wood, Feb 1884, F.W. Cragin 257 (NY00830462, syntype of *H. papillatum*); Pennsylvania, Allegheny Co., on dead wood, 14 Aug 1941, Henry, L.K. 4885 (BPI 591033); Pennsylvania, Meadville, old log, 17 Oct 1922, E.C. Smith 353 (BPI 591030); CANADA., on wood, J. Dearness (BPI 591035A, syntype of *H. papillatum*).

***Parahypoxylon ruwenzoriense* M. Cedeño-Sánchez, E. Charria-Girón & M. Stadler, sp. nov.**

MycoBank No: 845457

Figs 5–6

Holotype. DEMOCRATIC REPUBLIC OF THE CONGO. North Kivu: Mt. Ruwenzori, about 00°33.961'N, 29°81.795'E, between 2,138 and 2,400 m alt., 3–5 Feb 2008, tropical mountain forest, C. Decock (MUCL 51392, ex-holotype culture MUCL 51392).

Etymology. Named after the Ruwenzori Mountains, where the species was collected.

Teleomorph. Stromata superficial, incomplete, effused-pulvinate, 60 mm long × 40 mm broad × 3–5 mm thick; surface Fawn (87), with inconspicuous perithecial mounds, with a black, shiny hard crust 100–150 µm thick above perithecia, without visible granules, with KOH-extractable pigments Hazel (88); the pruina hyphae turn violet in KOH; the tissue below the perithecia 2–4 mm thick, vertically fibrose, dark grey. Perithecia tubular, 0.90–1.50 mm high × 0.2–0.3 mm diam (n=18). Ostioles umbilicate, surrounded by a white substance. Ascii cylindrical, 8-spored, the spore-bearing parts 82–105 µm long × 5.5–6.0 µm broad, the stipes 38–130 µm long, with amyloid, discoid apical ring 0.7–2.0 µm high × 2.5–3.5 µm (n=21) broad. Ascospores smooth, unicellular, brown to dark brown, narrowly ellipsoid, nearly equilateral with narrowly rounded ends, 10.5–13.8 × 4.0–5.6 µm (n=40), with a faint, straight germ slit; perispore indehiscent in 10% KOH.

Cultures and anamorph. Colonies on MEA, OA, and YM covering a 9 cm Petri plate in 2 weeks, with mycelium white at first, flat to raised in some zones, to becoming greenish in the center. Reverse at first yellowish, to become orange with a black spot at the center. Conidiophores not produced.

Secondary metabolites. Stromata contain BNT and cohaerin type azaphilones according to the MS/MS analysis.

Notes. *P. ruwenzoriense* is phylogenetically close to *P. papillatum* but differs by its KOH-extractable pigments Hazel (88) and by smaller ascospores.

Metabolomic profiling of stromata

As explained in the Experimental section, stromata of five herbarium specimens assignable to *Parahypoxylon* were extracted and analysed by UHPLC-DAD-IM-MS/MS. The raw data sets were pre-processed and the obtained feature table dereplicated using high resolution *m/z*, MS/MS spectra, retention time, CCS value, and UV/Vis spectra and reference data obtained from our in-house library of common secondary metabolites of the Hypoxylaceae (data not shown).

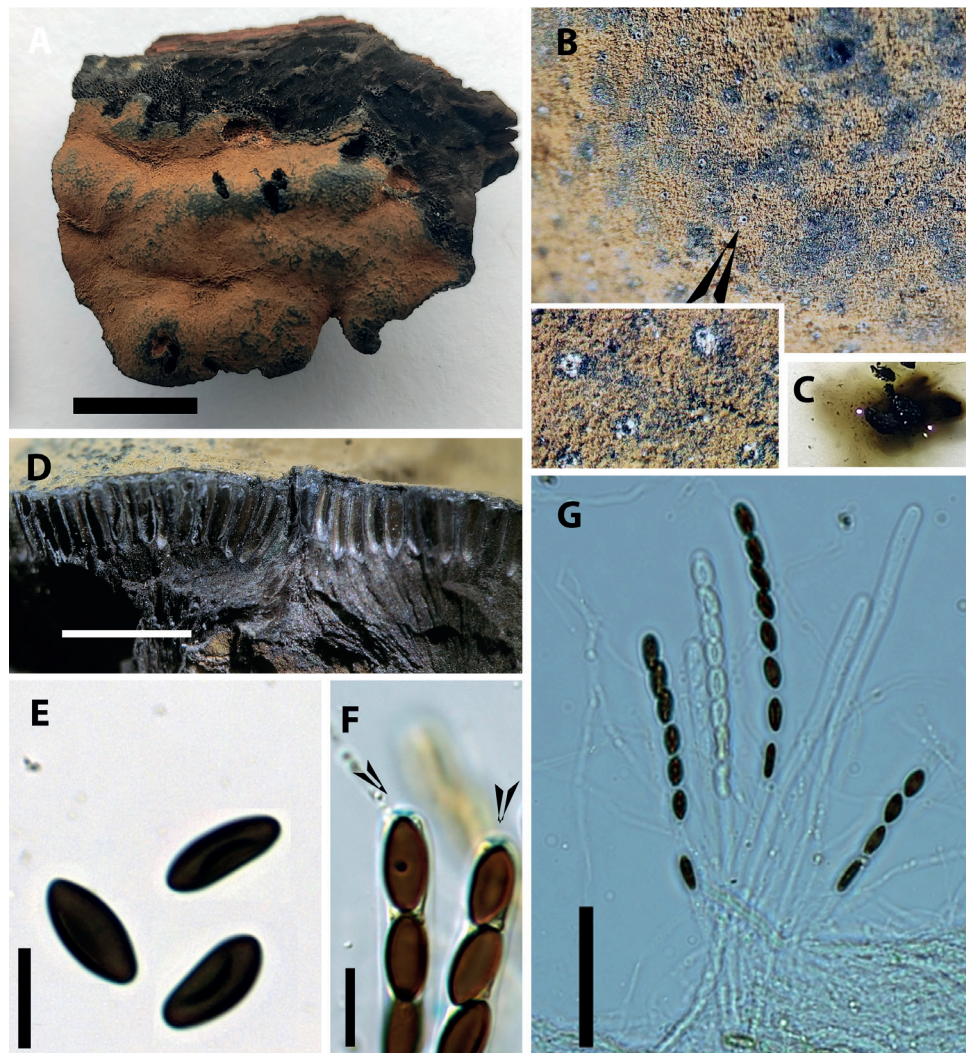


Figure 5. *Parahypoxylon ruwenzoriense* sp. nov. (MUCL 51392). **A** stroma **B** ostioles with white ring **C** KOH extractable stromatal pigments **D** perithecia (cross section) **E** ascospores **F** amyloid apical apparatus (blueing in Melzer's reagent) indicated by arrowheads **G** asci. Scale bars: 1 cm (**A**); 2 mm (**D**); 10 µm (**E, F**); 50 µm (**G**).

From the base peak chromatograms (BPC) of the stromatal extracts of the studied specimens, six major peaks could be distinguished (Fig. 7). An additional MS/MS similarity search without matching the precursor mass against our in-house library in MetaboScape yielded a MS/MS score > 700 for compounds **2** and **5** when compared with cohaerin E, cohaerin H, and minutellin A standards, which were not contained in the stromatal extracts (Suppl. material 1: fig. S2). This tentatively advocated

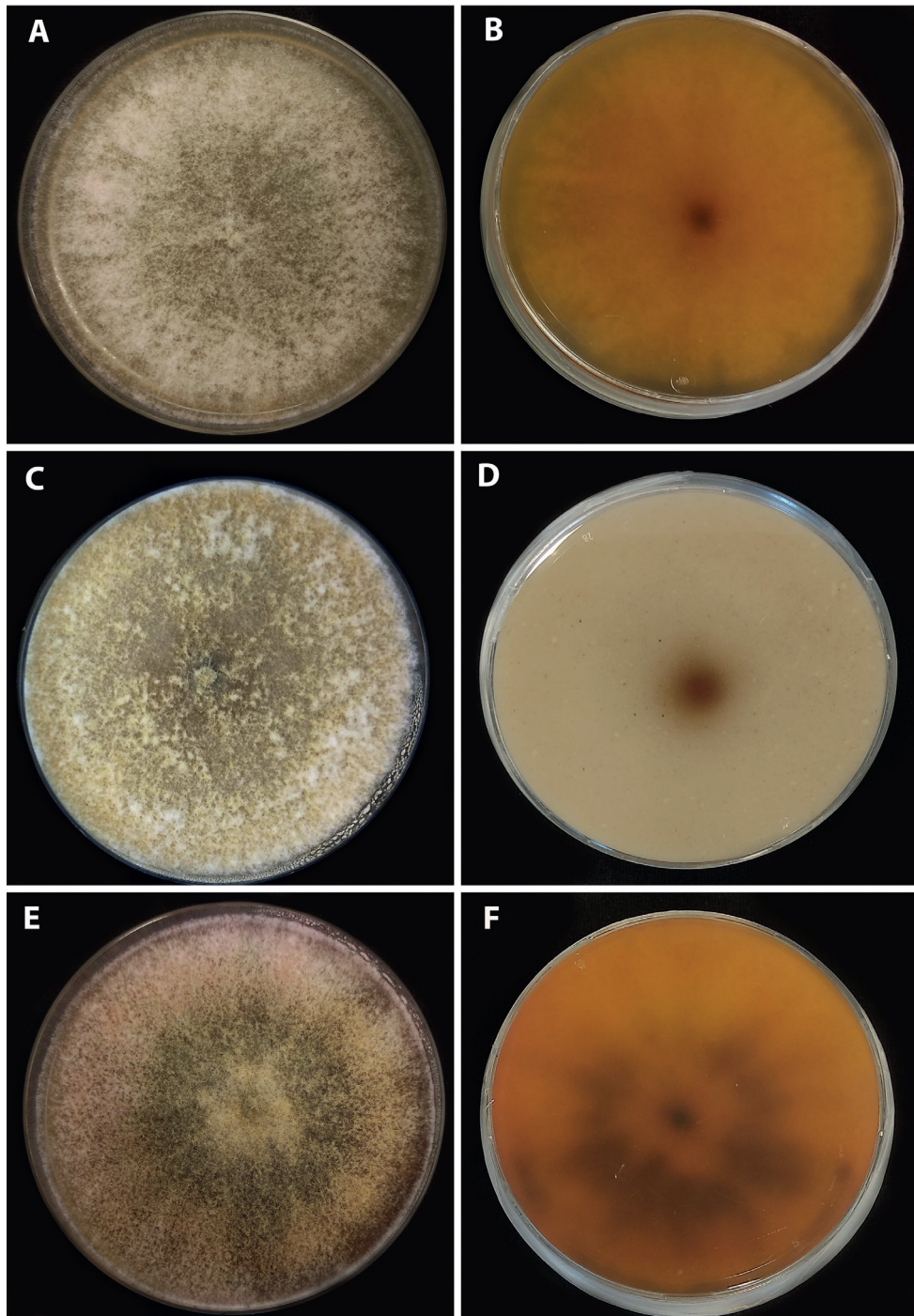


Figure 6. *Parahypoxylon ruwenzoriense* sp. nov. (MUCL 51392) Colonies after 2 weeks (**A, B**) on 2% MEA (**C, D**) on OA (**E, F**) on YM.

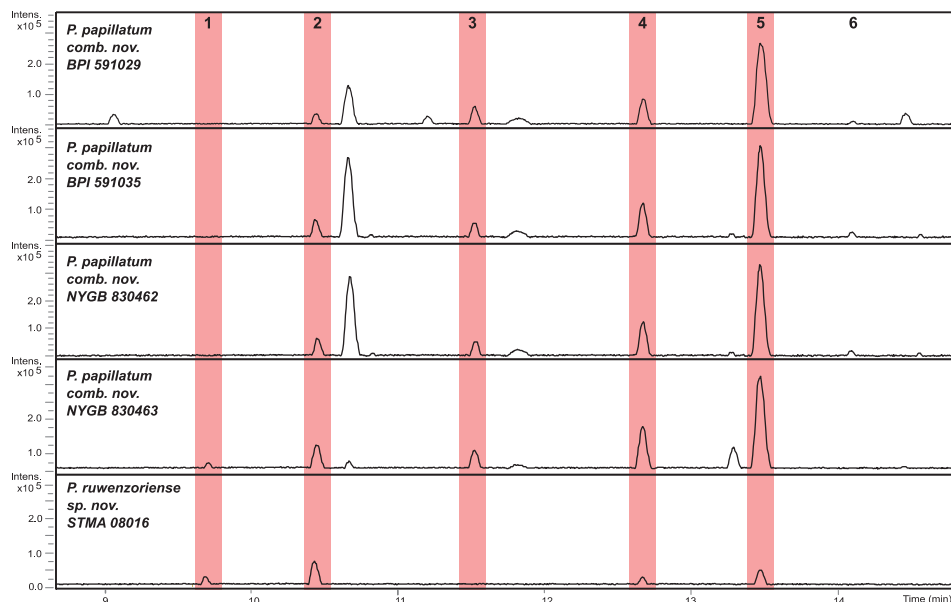


Figure 7. Base peak chromatograms (BPCs) from UHPLC-MS analysis of the stromatal extracts of *P. papillatum* (BPI 591029), *P. papillatum* (BPI 591035), *P. papillatum* (NYGB 830462), *P. papillatum* (NYGB 830463), and *Parahypoxylon ruwenzoriense* sp. nov. (STMA 08016). Compounds common between several species (numbered 1–6) are highlighted in red.

a structural relation to the azaphilone family (Fig. 8a). Molecular formulae for compounds **1–6** were predicted as $C_{23}H_{24}O_7$, $C_{23}H_{22}O_7$, $C_{23}H_{20}O_8$, $C_{23}H_{22}O_6$, $C_{23}H_{20}O_6$, and $C_{23}H_{21}NO_5$ (Suppl. material 1: table S7), with a lower number of carbons than cohaerin E ($C_{28}H_{30}O_6$), cohaerin H ($C_{28}H_{32}O_6$), and minutellin A ($C_{28}H_{30}O_7$). To further validate the presence of cohaerin E-like azaphilones in the stromatal extracts of the *Parahypoxylon* spp. a molecular networking (MN) approach was pursued. The above mentioned tool can be employed to organize in an automatic basis MS/MS spectra into groups based on similarities in their fragmentation patterns and the hypothesis that structurally related molecules will yield similar MS/MS spectra (Duncan et al. 2015). For this analysis, we compared the MS/MS spectra of cohaerin E, cohaerin H, and minutellin A (Suppl. material 1: table S7, fig. S2) with all MS/MS spectra obtained from the *Parahypoxylon* gen. nov. stromatal extracts by means of the unsupervised machine learning approach Spec2Vec. As a result, the molecular cluster containing the cohaerin standards consisted of 29 consensus spectra (nodes), which included compounds **1–6** (Fig. 8b). In addition, cohaerin E and H have UV/Vis absorptions at λ_{max} 226–223 and 344–380 nm, which are resembling UV/Vis absorptions from compounds **1, 3, 4**, and **6**. Minutellin A displayed UV/Vis absorptions at λ_{max} 224, 271, and 343 nm, a pattern identified also for compounds **2** and **5** (Fig. 8c).

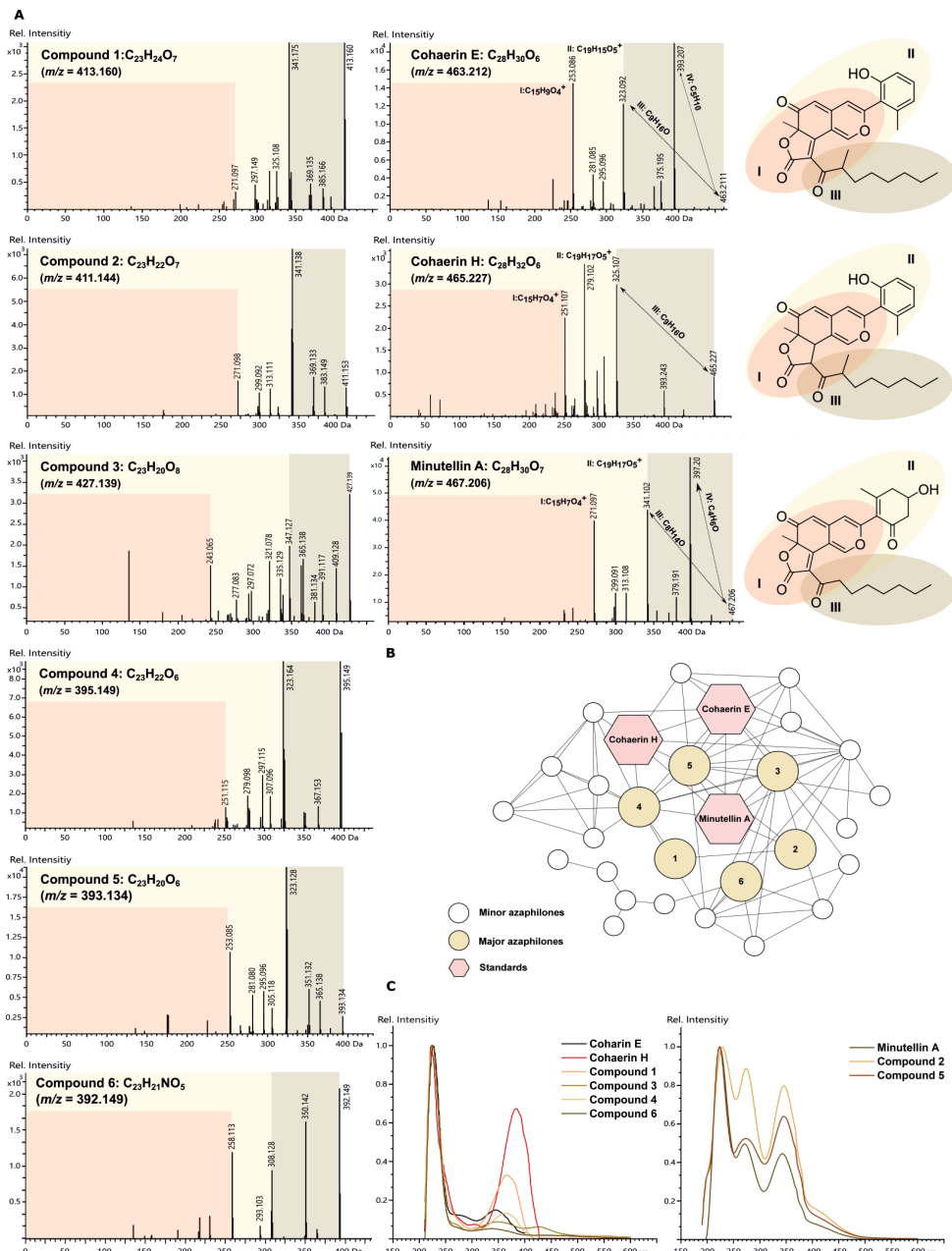


Figure 8. A Reference MS/MS spectra of cohaerin E, cohaerin H, and minutellin A standards, and the six major azaphilones identified in the UHPLC-MS chromatograms of stromatal extracts from the *Parahypoxylon* spp. **B** azaphilone cluster in a molecular network created from the *Parahypoxylon* spp. stromatal extracts and MS/MS spectra from selected standards **C** UV/Vis profile comparison from compound 1–6, cohaerin E, cohaerin H, and minutellin A.

Cohaerin-type azaphilones present as well a distinct MS fragmentation pattern. In MS/MS experiments, cohaerin E generated fragment ions at 393.207 Da, 323.092 Da, 281.085 Da, and 253.086 Da, while minutellin A generated fragment ions at 397.201 Da, 341.102 Da, 299.091 Da, and 271.097 Da. The most abundant fragments were annotated using the CFM-ID 4.0 peak assignment module. In both cases, the most abundant fragments were traced down to the azaphilone backbone (Fig. 9). For instance, the mass difference of 18 Da between 323.092 Da and 341.102 Da could be interpreted as H₂O, reflecting the different substitution of the 3-methylphenol moiety. Fragment ions at 281.085 Da and 253.086 Da for cohaerin E represent the tricyclic portion of the molecule, while fragment ions at 299.091 Da and 271.097 Da represent the same part of the molecule in minutellin A. Analogously, MS fragmentation patterns for cohaerin H (Fig. 8) resembles the generated fragments for cohaerin E. As some typical cohaerin-type azaphilones fragmentation patterns were conserved, we assume that the changes found for the stromatal metabolites of **1–6** occur in the side chain of the molecules. In summary, the UHPLC-DAD-IM-MS/MS and UV/Vis data, combined with a comparison of molecular networking analyses, indicated the presence of novel azaphilones related to the cohaerin family in the stromatal extracts from the *Parahypoxylon* spp., in contrast to the absence of other common secondary metabolites of the Hypoxylaceae.

Discussion

The genus *Hypoxylon* in the current taxonomic concept has frequently been shown to be paraphyletic (Wendt et al. 2018; Lambert et al. 2019), which has once more been confirmed in this study, foreshadowing again future rearrangements for a thorough revision of its systematics. This is especially apparent because the type species *H. fragiforme* forms a relatively small clade clustering with a small subset of closely related taxa. Therefore, further segregation will eventually be unavoidable once more data to safely delineate the different lineages becomes available. Here, we gathered chemotaxonomic, morphological and sequence data to enable a polyphasic characterization of a basal clade formerly phylogenetically resolved inside *Hypoxylon*, containing specimen closely related to *H. papillatum*, for which we propose the erection of the new genus *Parahypoxylon*, sharing many salient features with *Hypoxylon* in the “traditional” definition.

The investigation of the stromatal metabolite extracts by HPLC has proven to be a valuable resource to achieve a more natural classification of hypoxylaceous taxa (Kuhnert et al. 2015; Wendt et al. 2018; Lambert et al. 2019). Recent advances in the analytics for in-depth characterization of natural products, mainly driven by metabolomics-based strategies, have enabled a better understanding of complex natural systems (Van der Hooft et al. 2020). The current MS-based techniques can help as a predictor for the discovery of new carbon skeletons to help and prioritize their isolation

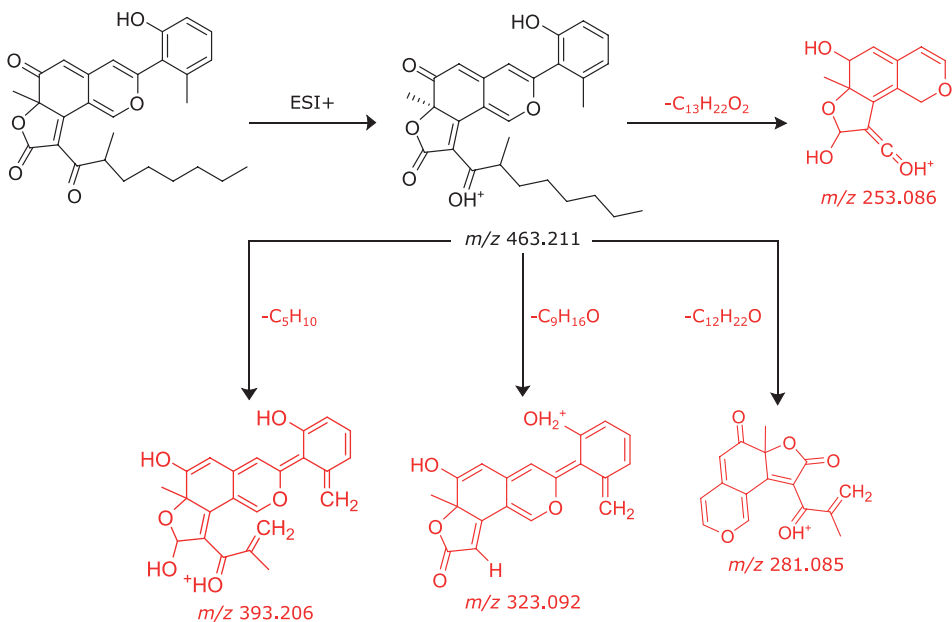
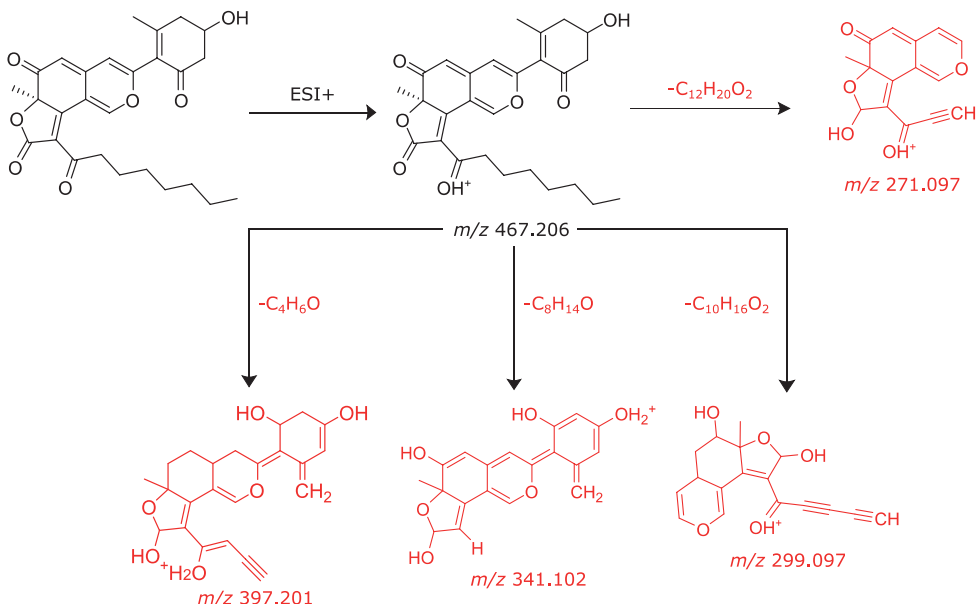
A**B**

Figure 9. **A** most abundant fragment ions observed in MS/MS spectra for cohaerin E and associated structures as predicted by CFM-ID 4.0 **B** most abundant fragment ions observed in MS/MS spectrum for minutellin A and associated structures as predicted by CFM-ID 4.0.

and description instead of the isolation of new derivatives of already known metabolite scaffolds. Nevertheless, relying mainly on MS/MS fragmentation spectra could lead to an underestimation of chemical diversity. The complex chemical space produced by a single BGC may result in completely different fragmentation patterns only by the addition of small structural changes (McCaughey et al. 2022). Still, a general methodology for characterizing and classifying structural analogs with a common biosynthetic origin is absent particularly in the field of fungal natural products (Almeida et al. 2020).

However, in many occasions and applications, the isolation and structure elucidation of yet unidentified compounds is not possible, such as in the example of isolating pigments from natural sources, as is the case in the genus *Hypoxyylon*. Even very old specimens have been reported to harbor intact secondary metabolites, as has been described for fossilized stromata assigned to *Hypoxyylon fragiforme* in a study of archeological samples by Surup et al. (2018). Here, fortunately the original species could be recollected in German woods, but for rarer specimens, or specimens only producing scarce amounts of stromata, this is not a practicable option. Instability of the contained metabolites during e.g. purification further complicates the issue (Stadler et al. 2008; Kuhnert et al. 2014b; Sir et al. 2019). In this study, we demonstrated the value of integrating metabolomics-based tools to characterize the secondary metabolite profile of the type and authentic specimens of *P. papillatum* and the new species from the D.R. Congo.

An MS/MS analysis of the major metabolites suggested the presence of six unknown compounds assignable to the azaphilones related to the cohaerin family, which have been predicted to harbor a smaller carbon skeleton than the known cohaerins, and which still conserve some of the distinctive fragmentation patterns of these secondary metabolites (Suppl. material 1: fig. S3). This phenomenon has been exemplified within the Hypoxylaceae, which present a highly diverse group of PKS-derived pigments, among which the different subfamilies present different attached side chains at the C-8 oxygen (Kuhnert et al. 2021). The above findings suggest that the type of azaphilone produced by the studied species belong to a different type of azaphilones with a shorter side chain, but with a shared backbone in comparison to the cohaerins and minutellins. Additionally, the number of nodes found in the MN analysis suggests that the chemical diversity of the azaphilones produced by the strains belonging to *Parahypoxyylon* gen. nov. is much higher than thought. In general, following a similar approach, the MolNetEnhancer workflow allowed the characterization of triterpenoid metabolites with several distinct phenolic acid modifications (e.g., vanillate, protocatechuate) in a different taxonomic background in the plant family Rhamnaceae (Ernst et al. 2019). The same methodology enabled the annotation of molecular families with known chemical motifs previously unreported for *Salinispora*, *Streptomyces*, and *Xenorhabdus* bacterial extracts (Ernst et al. 2019). Even though the ideal scenario would remain to isolate and elucidate the structures of the secondary metabolites, these tools are a powerful resource to classify chemical structural annotation and enhance our understanding of chemodiversity by adding biological and chemical insights of complex metabolic mixtures. It is worth noting that the stromatal material could eventually become available in the future from forthcoming collection campaigns, and

therefore the aforementioned hypothesis might be confirmed through isolation and chemical characterization of the major metabolites.

In this context, the stromatal metabolite profile of the specimens of *P. papillatum* and the new species *P. ruwenzoriense* are rather unique, even though it exhibits related chemotaxonomic features more likely to be found in the Hypoxylaceae. The cohaerin type azaphilones (which include also the multiformins and minutellins) have first been reported by Quang et al. (2005a, b, 2006), Surup et al. (2013) and Kuhnert et al. (2017b) and were recently found to possess interesting antiviral effects (Jansen-Olliges et al. 2023). Their producers are now all classified in *Jackrogersella* (Wendt et al. 2018) and were formerly placed in *Hypoxylon* sect. *Annulata* or (Ju and Rogers 1996) *Annulohypoxylon* (Hsieh et al. 2005), respectively. Kuhnert et al. (2017a) already reported that the species of *Annulohypoxylon* are divided into two chemotypes, one of which is characterized by stromata with papillate ostioles and cohaerin type azaphilones. The other chemotype is devoid of these compounds and produces binaphthalenes as prevailing stromatal metabolites. It includes *A. truncatum*, the type species of *Annulohypoxylon*, and many other species that feature ostiolar discs. Since this coincided with the molecular phylogeny by Wendt et al. (2018), the new genus *Jackrogersella* was erected for the cohaerin-containing species with papillate, diskless ostioles. There is only one species in *Annulohypoxylon* (i.e., *A. michelianum*) that has such ostiolar rings and also produces cohaerins. It was left at interim in *Annulohypoxylon*, even though its DNA sequence occupied a separate clade in the phylogeny by Wendt et al. (2018). The reason is that the strain studied did not constitute type material, and we felt that the erection of a separate genus should only be carried out by including fresh material from the geographic area and host (*Laurus* in South Europe) from which the holotype specimen was reported. Aside from the above-mentioned fungi, metabolites with cohaerin-like characteristics (i.e. characteristic mass and diode array spectra) have even been detected in species of *Hypoxylon*, such as *H. pulicidum* (Bills et al. 2012). A recent study based on the analysis of full genomes based on 3rd generation sequencing techniques, such as PacBio and Oxford nanopore (Wibberg et al. 2021), has even revealed the corresponding biosynthetic gene clusters encoding for these azaphilone pigments to be present in the studied *Jackrogersella* species and *H. pulicidum* (Kuhnert et al. 2021). For instance, the identified BGC in *H. pulicidum* carries the core set of conserved genes for this family of azaphilones, but the additional presence of additional tailoring enzymes indicates that the produced metabolites might have different structural features compared to the known cohaerins (Kuhnert et al. 2021).

In the future, it will become easier to tell if the genetic information for the successful biosynthesis of such secondary metabolites is present in the genomes of the respective organisms even if the products cannot be detected. Chemotaxonomic evidence can also be used to segregate the new genus from the species that are located in neighboring basal clades in the current phylogeny (i.e., *Hypoxylon aeruginosum* and *Durotheca* spp.). Interestingly, these species neither contain azaphilones nor binaphthalenes, with *H. aeruginosum* and the related genus *Chlorostroma* reported to have lepraric acid derivatives as major stromatal metabolites (Læssøe et al. 2010), which are

otherwise unique and only occur in some lichenized ascomycetes. *Durotheca*, on the other hand, appears to be poor in stromatal metabolites, and Læssøe et al. (2013) only found traces of lepraric acids in one of the species they studied. The current study has further confirmed the results by de Long et al. (2019), who found that *Durotheca* is a hypoxylaceous genus, even though its species have a distinctive ascospore morphology and other secondary metabolites.

The integration of state-of-the-art metabolomic-based tools in chemotaxonomic surveys will further accelerate and assist the systematic study of paraphyletic taxa within the concept of polyphasic taxonomy as herein demonstrated for the introduction of *Parahypoxylon*.

Acknowledgements

This work was funded by the DFG (Deutsche Forschungsgemeinschaft) priority program “Taxon-Omics: New Approaches for Discovering and Naming Biodiversity” (SPP 1991). It also benefited from the European Union’s H2020 Research and Innovation Staff Exchange program (RISE) [Grant No. 101008129: MYCOBIOMICS], granted to J.J. Luangsa-ard and M. Stadler. MCS gratefully acknowledges a PhD stipend from The National Secretariat of Science, Technology and Innovation of the Republic of Panama (SENACYT) and the Institute for the Development of Human Resources (IFARHU). E. Charria-Girón was funded by the HZI POF IV Cooperativity and Creativity Project Call. Additionally, we gratefully acknowledge support from the curators of the international herbaria, above all Lisa A Castlebury (BPI), Laura Briscoe (NY) and Monique Slipher (WSP), who provided important specimens for this study. Additionally, we are grateful for the expert and technical advice from Ulrike Beutling and Frank Surup.

References

- Almeida H, Palys S, Tsang A, Diallo AB (2020) TOUCAN: A framework for fungal biosynthetic gene cluster discovery. NAR Genomics and Bioinformatics 2(4): 1–11. <https://doi.org/10.1093/nargab/lqa098>
- Anisimova M, Gil M, Dufayard JF, Dessimoz C, Gascuel O (2011) Survey of branch support methods demonstrates accuracy, power, and robustness of fast likelihood-based approximation schemes. Systematic Biology 60(5): 685–699. <https://doi.org/10.1093/sysbio/syr041>
- Becker K, Stadler M (2021) Recent progress in biodiversity research on the Xylariales and their secondary metabolism. The Journal of Antibiotics 74(1): 1–23. <https://doi.org/10.1038/s41429-020-00376-0>
- Becker K, Lambert C, Wieschhaus J, Stadler M (2020) Phylogenetic assignment of the fungi-colous *Hypoxylon invadens* (Ascomycota, Xylariales) and investigation of its secondary metabolites. Microorganisms 8(9): 1397. <https://doi.org/10.3390/microorganisms8091397>

- Bills GF, González-Menéndez V, Martín J, Platas G, Fournier J, Peršoh D, Stadler M (2012) *Hypoxyton pulicidum* sp. nov. (Ascomycota, Xylariales), a pantropical insecticide-producing endophyte. PLoS ONE 7(10): e46687. <https://doi.org/10.1371/journal.pone.0046687>
- Bitzer J, Læssøe T, Fournier J, Kummer V, Decock C, Tichy H-V, Piepenbring M, Peršoh D, Stadler M (2008) Affinities of *Phylacia* and the daldinoid Xylariaceae, inferred from chemotypes of cultures and ribosomal DNA sequences. Mycological Research 112(2): 251–270. <https://doi.org/10.1016/j.mycres.2007.07.004>
- Cedeño-Sánchez M, Wendt L, Stadler M, Mejía LC (2020) Three new species of *Hypoxyton* and new records of Xylariales from Panama. Mycosphere 11(1): 1457–1476. <https://doi.org/10.5943/mycosphere/11/1/9>
- Chernomor O, Von Haeseler A, Minh BQ (2016) Terrace aware data structure for phylogenomic inference from supermatrices. Systematic Biology 65(6): 997–1008. <https://doi.org/10.1093/sysbio/syw037>
- Daranagama DA, Camporesi E, Tian Q, Liu X, Chamyuang S, Stadler M, Hyde KD (2015) *Anthostomella* is polyphyletic comprising several genera in Xylariaceae. Fungal Diversity 73(1): 203–238. <https://doi.org/10.1007/s13225-015-0329-6>
- Daranagama DA, Hyde KD, Sir EB, Thambugala KM, Tian Q, Samarakoon MC, McKenzie EHC, Jayasiri SC, Tibpromma S, Bhat JD, Liu X, Stadler M (2018) Towards a natural classification and backbone tree for Graphostromataceae, Hypoxylaceae, Lopadostomataceae and Xylariaceae. Fungal Diversity 88(1): 1–165. <https://doi.org/10.1007/s13225-017-0388-y>
- de Long Q, Liu LL, Zhang X, Wen TC, Kang JC, Hyde KD, Shen XC, Li QR (2019) Contributions to species of Xylariales in China-1. *Durotheca* species. Mycological Progress 18(3): 495–510. <https://doi.org/10.1007/s11557-018-1458-6>
- Duncan KR, Crüsemann M, Lechner A, Sarkar A, Li J, Ziemert N, Wang M, Bandeira N, Moore BS, Dorrestein PC, Jensen PR (2015) Molecular networking and pattern-based genome mining improves discovery of biosynthetic gene clusters and their products from *Salinispora* species. Chemistry & Biology 22(4): 460–471. <https://doi.org/10.1016/j.chembiol.2015.03.010>
- Ernst M, Kang K, Caraballo-Rodríguez AM, Nothias L-F, Wandy J, Chen C, Wang M, Rogers S, Medema MH, Dorrestein PC, van der Hooft JJJ (2019) Molnetenhancer: Enhanced molecular networks by integrating metabolome mining and annotation tools. Metabolites 9(7): 144. <https://doi.org/10.3390/metabo9070144>
- Felsenstein J (1985) Confidence limits on phylogenies: An approach using the bootstrap. Evolution 39(4): 783–791. <https://doi.org/10.2307/2408678>
- Fournier J, Köpcke B, Stadler M (2010a) New species of *Hypoxyton* from western Europe and Ethiopia. Mycotaxon 113(1): 209–235. <https://doi.org/10.5248/113.209>
- Fournier J, Stadler M, Hyde KD, Duong LM (2010b) The new genus *Rostrohypoxyton* and two new *Annulohypoxyton* species from Northern Thailand. Fungal Diversity 40(1): 23–36. <https://doi.org/10.1007/s13225-010-0026-4>
- Fournier J, Flessa F, Peršoh D, Stadler M (2011) Three new *Xylaria* species from Southwestern Europe. Mycological Progress 10(1): 33–52. <https://doi.org/10.1007/s11557-010-0671-8>
- Friebes G, Wendelin I (2016) Studies on *Hypoxyton ferrugineum* (Xylariaceae), a rarely reported species collected in the urban area of Graz (Austria). Ascomycete.org 8: 83–90.

- Helaly SE, Thongbai B, Stadler M (2018) Diversity of biologically active secondary metabolites from endophytic and saprotrophic fungi of the ascomycete order Xylariales. *Natural Product Reports* 35(9): 992–1014. <https://doi.org/10.1039/C8NP00010G>
- Heredia G, Li DW, Wendt L, Réblová M, Arias RM, Gamboa-Angulo M, Štěpánek V, Stadler M, Castañeda-Ruiz RF (2020) *Natonodosa speciosa* gen. et sp. nov. and rediscovery of *Poroisariopsis inornata*: Neotropical anamorphic fungi in Xylariales. *Mycological Progress* 19(1): 15–30. <https://doi.org/10.1007/s11557-019-01537-8>
- Hsieh H-M, Ju Y-M, Rogers JD (2005) Molecular phylogeny of *Hypoxyylon* and closely related genera. *Mycologia* 97(4): 844–865. <https://doi.org/10.1080/15572536.2006.11832776>
- Hsieh H-M, Lin C-R, Fang M-J, Rogers JD, Fournier J, Lechat C, Ju Y-M (2010) Phylogenetic status of *Xylaria* subgenus *Pseudoxylaria* among taxa of the subfamily Xylarioideae (Xylariaceae) and phylogeny of the taxa involved in the subfamily. *Molecular Phylogenetics and Evolution* 54(3): 957–969. <https://doi.org/10.1016/j.ympev.2009.12.015>
- Huber F, Ridder L, Verhoeven S, Spaaks JH, Diblen F, Rogers S, Van Der Hooft JJJ (2021) Spec2Vec: Improved mass spectral similarity scoring through learning of structural relationships. *PLoS Computational Biology* 17(2): e1008724. <https://doi.org/10.1371/journal.pcbi.1008724>
- Hyde K, Norphanphoun C, Maharachchikumbura SSN, Bhat DJ, Jones EBG, Bundhun D, Chen YJ, Bao DF, Boonmee S, Calabon MS, Chaiwan N, Chethana KWT, Dai DQ, Darayathne MC, Devadatha B, Dissanayake AJ, Dissanayake LS, Doilom M, Dong W, Fan XL30, Goonasekara ID, Hongsanan S, Huang SK, Jayawardena RS, Jeewon R, Karunarathna A, Konta S, Kumar V, Lin CG, Liu JK, Liu NG, Luangsa-ard J, Lumyong S, Luo ZL, Marasinghe DS, McKenzie EHC, Niego AGT, Niranjan M, Perera RH, Phukhamsakda C, Rathnayaka AR, Samarakoon MC, Samarakoon SMBC, Sarma VV, Senanayake IC, Shang QJ, Stadler M, Tibpromma S, Wanasinghe DN, Wei DP, Wijayawardene NN, Xiao YP, Yang J, Zeng XY, Zhang SN, Xiang MM (2020) Refined families of Sordariomycetes. *Mycosphere* 11(1): 305–1059. <https://doi.org/10.5943/mycosphere/11/1/7>
- Jansen-Olliges L, Chatterjee S, Jia L, Stahl F, Bär C, Stadler M, Surup F, Zeilinger C (2022) Coherin-type azaphilones prevent SARS-CoV-2 binding to ACE2 receptor. *Cells* 12(1): 83. <https://doi.org/10.3390/cells12010083>
- Ju Y, Rogers JD (1996) A revision of the genus *Hypoxyylon*. *Mycologia Memoir No. 20*. American Phytopathological Society, APS Press.
- Ju Y-M, Rogers JD, Hsieh H-M (2003) The genus *Theissenia*: *T. pyrenocrata*, *T. cinerea* sp. nov., and *T. eurima* sp. nov. *Mycologia* 95(1): 109–116. <https://doi.org/10.1080/15572536.2004.11833138>
- Ju Y-M, Hsieh H-M, Ho M-C, Szu D-H, Fang M-J (2007) *Theissenia rogersii* sp. nov. and phylogenetic position of *Theissenia*. *Mycologia* 99(4): 612–621. <https://doi.org/10.1080/15572536.2007.11832555>
- Kalyaanamoorthy S, Minh BQ, Wong TKF, von Haeseler A, Jermiin LS (2017) ModelFinder: Fast model selection for accurate phylogenetic estimates. *Nature Methods* 14(6): 587–589. <https://doi.org/10.1038/nmeth.4285>
- Katoh K, Rozewicki J, Yamada KD (2019) MAFFT online service: Multiple sequence alignment, interactive sequence choice and visualization. *Briefings in Bioinformatics* 20(4): 1160–1166. <https://doi.org/10.1093/bib/bbx108>

- Kearse M, Moir R, Wilson A, Stones-Havas S, Cheung M, Sturrock S, Buxton S, Cooper A, Markowitz S, Duran C, Thierer T, Ashton B, Meintjes P, Drummond A (2012) Geneious Basic: An integrated and extendable desktop software platform for the organization and analysis of sequence data. *Bioinformatics* 28(12): 1647–1649. <https://doi.org/10.1093/bioinformatics/bts199>
- Koukol O, Kelnarová I, Černý K (2015) Recent observations of sooty bark disease of sycamore maple in Prague (Czech Republic) and the phylogenetic placement of *Cryptostroma corticale*. *Forest Pathology* 45(1): 21–27. <https://doi.org/10.1111/efp.12129>
- Kuhnert E, Heitkämper S, Fournier J, Surup F, Stadler M (2014a) Hypoxyvermelhotins A–C, new pigments from *Hypoxyylon lechatii* sp. nov. *Fungal Biology* 118(2): 242–252. <https://doi.org/10.1016/j.funbio.2013.12.003>
- Kuhnert E, Fournier J, Peršoh D, Luangsa-ard JJD, Stadler M (2014b) New *Hypoxyylon* species from Martinique and new evidence on the molecular phylogeny of *Hypoxyylon* based on ITS rDNA and β-tubulin data. *Fungal Diversity* 64(1): 181–203. <https://doi.org/10.1007/s13225-013-0264-3>
- Kuhnert E, Surup F, Sir EB, Lambert C, Hyde KD, Hladki AI, Romero AI, Stadler M (2015) Lenormandins A—G, new azaphilones from *Hypoxyylon lenormandii* and *Hypoxyylon jaklitschii* sp. nov., recognised by chemotaxonomic data. *Fungal Diversity* 71(1): 165–184. <https://doi.org/10.1007/s13225-014-0318-1>
- Kuhnert E, Sir EB, Lambert C, Hyde KD, Hladki AI, Romero AI, Rohde M, Stadler M (2017a) Phylogenetic and chemotaxonomic resolution of the genus *Annulohypoxyylon* (Xylariaceae) including four new species. *Fungal Diversity* 85(1): 1–43. <https://doi.org/10.1007/s13225-016-0377-6>
- Kuhnert E, Surup F, Halecker S, Stadler M (2017b) Minutellins A – D, azaphilones from the stromata of *Annulohypoxyylon minutellum* (Xylariaceae). *Phytochemistry* 137: 67–71. <https://doi.org/10.1016/j.phytochem.2017.02.014>
- Kuhnert E, Navarro-Muñoz JC, Becker K, Stadler M, Collemare J, Cox RJ (2021) Secondary metabolite biosynthetic diversity in the fungal family Hypoxylaceae and *Xylaria hypoxylon*. *Studies in Mycology* 99(1): 100118. <https://doi.org/10.1016/j.simyco.2021.100118>
- Læssøe T, Srikitkulchai P, Fournier J, Köpcke B, Stadler M (2010) Lepraric acid derivatives as chemotaxonomic markers in *Hypoxyylon aeruginosum*, *Chlorostroma subcubisporum* and *C. cyaninum*, sp. nov. *Fungal Biology* 114(5–6): 481–489. <https://doi.org/10.1016/j.funbio.2010.03.010>
- Læssøe T, Srikitkulchai P, Luangsa-ard JJD, Stadler M (2013) *Theissenia* reconsidered, including molecular phylogeny of the type species *T. pyrenocystata* and a new genus *Durothecea* (Xylariaceae, Ascomycota). *IMA Fungus* 4(1): 57–69. <https://doi.org/10.5598/imafungus.2013.04.01.07>
- Lambert C, Wendt L, Hladki AI, Stadler M, Sir EB (2019) *Hypomontagnella* (Hypoxylaceae): A new genus segregated from *Hypoxyylon* by a polyphasic taxonomic approach. *Mycological Progress* 18(1–2): 187–201. <https://doi.org/10.1007/s11557-018-1452-z>
- Lambert C, Pourmoghaddam MJ, Cedeño-Sánchez M, Surup F, Khodaparast SA, Krisai-Greilhuber I, Voglmayr H, Stradal TEB, Stadler M (2021) Resolution of the *Hypoxyylon fuscum* complex (Hypoxylaceae, Xylariales) and discovery and biological characterization of two of its prominent secondary metabolites. *Journal of Fungi* 7(2): 131. <https://doi.org/10.3390/jof7020131>

- Lanfear R, Frandsen PB, Wright AM, Senfeld T, Calcott B (2016) PartitionFinder 2: New methods for selecting partitioned models of evolution for molecular and morphological phylogenetic analyses. *Molecular Biology and Evolution* 34: 772–773. <https://doi.org/10.1093/molbev/msw260>
- Liu YJ, Whelen S, Hall BD (1999) Phylogenetic relationships among ascomycetes: Evidence from an RNA polymerase II subunit. *Molecular Biology and Evolution* 16(12): 1799–1808. <https://doi.org/10.1093/oxfordjournals.molbev.a026092>
- Ma H, Song Z, Pan X, Li Y, Yang Z, Qu Z (2022) Multi-gene phylogeny and taxonomy of *Hypoxyylon* (Hypoxylaceae, Ascomycota) from China. *Diversity (Basel)* 14(1): 37. <https://doi.org/10.3390/d14010037>
- Matio Kemkuignou B, Schweizer L, Lambert C, Anoumedem EGM, Kouam SF, Stadler M, Marin-Felix Y (2022) New polyketides from the liquid culture of *Diaporthe breyniae* sp. nov. (Diaporthales, Diaporthaceae). *MycoKeys* 90: 85–118. <https://doi.org/10.3897/mycokeys.90.82871>
- McCaughey CS, van Santen JA, van der Hooft JJJ, Medema MH, Linington RG (2022) An isotopic labeling approach linking natural products with biosynthetic gene clusters. *Nature Chemical Biology* 18(3): 295–304. <https://doi.org/10.1038/s41589-021-00949-6>
- Miller JH (1961) A monograph of the world species of *Hypoxyylon*. Univ. Georgia Press, Athens, 158 pp.
- Minh BQ, Schmidt HA, Chernomor O, Schrempf D, Woodhams MD, von Haeseler A, Lanfear R (2020) IQ-TREE 2: New models and efficient methods for phylogenetic inference in the genomic era. *Molecular Biology and Evolution* 37(5): 1530–1534. <https://doi.org/10.1093/molbev/msaa015>
- Nothias LF, Petras D, Schmid R, Dührkop K, Rainer J, Sarvepalli A, Protsyuk I, Ernst M, Tsugawa H, Fleischauer M, Aicheler F, Aksenen AA, Alka O, Allard PM, Barsch A, Cachet X, Caraballo-Rodriguez AM, Da Silva RR, Dang T, Garg N, Gauglitz JM, Gurevich A, Isaac G, Jarmusch AK, Kameník Z, Kang K, Kessler N, Koester I, Korf A, Le Gouellec A, Ludwig M, Martin H C, McCall L-I, McSayles J, Meyer SW, Mohimani H, Morsy M, Moyne O, Neumann S, Neuweiler H, Nguyen NH, Nothias-Esposito M, Paolini J, Phelan VV, Pluskal T, Quinn RA, Rogers S, Shrestha B, Tripathi A, van der Hooft JJJ, Vargas F, Weldon KC, Witting M, Yang H, Zhang Z, Zubeil F, Kohlbacher O, Böcker S, Alexandrov T, Bandeira N, Wang M, Dorrestein PC (2020) Feature-based molecular networking in the GNPS analysis environment. *Nature Methods* 17(9): 905–908. <https://doi.org/10.1038/s41592-020-0933-6>
- O'Donnell K, Cigelnik E (1997) Two divergent intragenomic rDNA ITS2 types within a monophyletic lineage of the fungus *Fusarium* are nonorthologous. *Molecular Phylogenetics and Evolution* 7(1): 103–116. <https://doi.org/10.1006/mpev.1996.0376>
- Pourmoghaddam MJ, Lambert C, Surup F, Khodaparast SA, Krisai-Greilhuber I, Voglmayr H, Stadler M (2020) Discovery of a new species of the *Hypoxyylon rubiginosum* complex from Iran and antagonistic activities of *Hypoxyylon* spp. against the Ash Dieback pathogen, *Hymenoscyphus fraxineus*, in dual culture. *MycoKeys* 66: 105–133. <https://doi.org/10.3897/mycokeys.66.50946>
- Quang DN, Hashimoto T, Nomura Y, Wollweber H, Hellwig V, Fournier J, Stadler M, Asakawa Y (2005a) Cohaerins A and B, azaphilones from the fungus *Hypoxyylon cohaerens*,

- and comparison of HPLC-based imetabolite profiles in *Hypoxyton* sect. *Annulata*. *Phytochemistry* 66: 797–809. 1 <https://doi.org/10.1016/j.phytochem.2005.02.006>
- Quang DN, Hashimoto T, Stadler M, Radulović N, Asakawa Y (2005b) Antimicrobial azaphilones from the fungus *Hypoxyton multifforme*. *Planta Medica* 71(11): 1058–1062. <https://doi.org/10.1055/s-2005-873129>
- Quang DN, Stadler M, Fournier J, Tomita A, Hashimoto T (2006) Cohaeirins C–F, four azaphilones from the xylariaceous fungus *Annulohypoxyton cohaerens*. *Tetrahedron* 62(26): 6349–6354. <https://doi.org/10.1016/j.tet.2006.04.040>
- Rayner RW (1970) A Mycological Colour Chart. Commonwealth Mycological Institute, Kew and British Mycological Society.
- Rogers J (1985) *Hypoxyton duranii* sp. nov. and the anamorphs of *H. caries*, *H. papillatum*, and *Rosellinia subiculata*. *Mycotaxon* 23: 429–437.
- Ronquist F, Teslenko M, van der Mark P, Ayres DL, Darling A, Höhna S, Larget B, Liu L, Suchard MA, Huelsenbeck JP (2012) MrBayes 3.2: Efficient Bayesian Phylogenetic Inference and model choice across a large model space. *Systematic Biology* 61(3): 539–542. <https://doi.org/10.1093/sysbio/sys029>
- Shimodaira H (2022) An approximately unbiased test of phylogenetic tree selection. *Systematic Biology* 51(3): 492–508. <https://doi.org/10.1080/10635150290069913>
- Sir EB, Kuhnert E, Surup F, Hyde KD, Stadler M (2015) Discovery of new mitorubrin derivatives from *Hypoxyton fulvo-sulphureum* sp. nov. (Ascomycota, Xylariales). *Mycological Progress* 14(5): 28. <https://doi.org/10.1007/s11557-015-1043-1>
- Sir EB, Kuhnert E, Lambert C, Hladki AI, Romero AI, Stadler M (2016) New species and reports of *Hypoxyton* from Argentina recognized by a polyphasic approach. *Mycological Progress* 15(4): 42. <https://doi.org/10.1007/s11557-016-1182-z>
- Sir EB, Becker K, Lambert C, Bills GF, Kuhnert E (2019) Observations on Texas hypoxylons, including two new *Hypoxyton* species and widespread environmental isolates of the *H. croceum* complex identified by a polyphasic approach. *Mycologia* 111(5): 832–856. <https://doi.org/10.1080/00275514.2019.1637705>
- Smith CL (1893) Some Central American Pyrenomycetes. *Bulletin from the laboratories of natural history of the State University of Iowa* 2: 408.
- Stadler M, Fournier J, Granmo A, Beltrán-Tejera E (2008) The “red Hypoxylons” of the temperate and subtropical Northern hemisphere. *North American Fungi* 3: 73–125. <https://doi.org/10.2509/naf2008.003.0075>
- Stadler M, Fournier J, Læssøe T, Chlebicki A, Lechat C, Flessa F, Rambold G, Peršoh D (2010) Chemotaxonomic and phylogenetic studies of *Thamnomyces* (Xylariaceae). *Mycoscience* 51(3): 189–207. <https://doi.org/10.1007/S10267-009-0028-9>
- Stadler M, Kuhnert E, Peršoh D, Fournier J (2013) The Xylariaceae as model example for a unified nomenclature following the “One Fungus-One Name” (1F1N) concept. *Mycology* 4: 5–21. <https://doi.org/10.1080/21501203.2013.782478>
- Stadler M, Læssøe T, Fournier J, Decock C, Schmieschek B, Tichy H-V, Peršoh D (2014) A polyphasic taxonomy of *Daldinia* (Xylariaceae) 1. *Studies in Mycology* 77: 1–143. <https://doi.org/10.3114/sim0016>
- Stadler M, Lambert C, Wibberg D, Kalinowski J, Cox RJ, Kolařík M, Kuhnert E (2020) Intron genomic polymorphisms in the ITS region of high-quality genomes of the Hypoxylaceae

- (Xylariales, Ascomycota). *Mycological Progress* 19(3): 235–245. <https://doi.org/10.1007/s11557-019-01552-9>
- Surup F, Mohr KI, Jansen R, Stadler M (2013) Cohaerins G–K, azaphilone pigments from *Annulohypoxylon cohaerens* and absolute stereochemistry of cohaerins C–K. *Phytochemistry* 95: 252–258. <https://doi.org/10.1016/j.phytochem.2013.07.027>
- Surup F, Narmani A, Wendt L, Pfütze S, Kretz R, Becker K, Menbrivès C, Giosa A, Elliott M, Petit C, Rohde M, Stadler M (2018) Identification of fungal fossils and novel azaphilone pigments in ancient carbonised specimens of *Hypoxylon fragiforme* from forest soils of Châtillon-sur-Seine (Burgundy). *Fungal Diversity* 92(1): 345–356. <https://doi.org/10.1007/s13225-018-0412-x>
- Tang A, Jeewon R, Hyde KD (2009) A re-evaluation of the evolutionary relationships within the Xylariaceae based on ribosomal and protein-coding gene sequences. *Fungal Diversity* 34: 127–155.
- Tamura K, Stecher G, Kumar S (2021) MEGA11: Molecular evolutionary genetics analysis Version 11. *Molecular Biology and Evolution* 38(7): 3022–3027. <https://doi.org/10.1093/molbev/msab120>
- Tian DS, Kuhnert E, Ouazzani J, Wibberg D, Kalinowski J, Cox RJ (2020) The sporothriolides. A new biosynthetic family of fungal secondary metabolites. *Chemical Science* 11(46): 12477–12484. <https://doi.org/10.1039/D0SC04886K>
- Triebel D, Peršoh D, Wollweber H, Stadler M (2005) Phylogenetic relationships among *Daldinia*, *Entonaema* and *Hypoxylon* as inferred from ITS nrDNA analyses of Xylariales. *Nova Hedwigia* 80(1–2): 25–43. <https://doi.org/10.1127/0029-5035/2005/0080-0025>
- U'Ren JM, Miadlikowska J, Zimmerman NB, Lutzoni F, Stajich JE, Arnold AE, U'Ren JM (2016) Contributions of North American endophytes to the phylogeny, ecology, and taxonomy of Xylariaceae (Sordariomycetes, Ascomycota). *Molecular Phylogenetics and Evolution* 98: 210–232. <https://doi.org/10.1016/j.ympev.2016.02.010>
- Van der Hooft JJJ, Mohimani H, Bauermeister A, Dorrestein PC, Duncan KR, Medema MH (2020) Linking genomics and metabolomics to chart specialized metabolic diversity. *Chemical Society Reviews* 49(11): 3297–3314. <https://doi.org/10.1039/D0CS00162G>
- Vicente TFL, Gonçalves MFM, Brandão C, Fidalgo C, Alves A (2021) Diversity of fungi associated with macroalgae from an estuarine environment and description of *Cladosporium rubrum* sp. nov. and *Hypoxylon aveirense* sp. nov. *International Journal of Systematic and Evolutionary Microbiology* 71(2): 004630. <https://doi.org/10.1099/ijsem.0.004630>
- Vilgalys R, Hester M (1990) Rapid genetic identification and mapping of enzymatically amplified ribosomal DNA from several *Cryptococcus* species. *Journal of Bacteriology* 172(8): 4238–4246. <https://doi.org/10.1128/jb.172.8.4238-4246.1990>
- Vu D, Groenewald M, de Vries M, Gehrmann T, Stielow B, Eberhardt U, Al-Hatmi A, Groenewald JZ, Cardinali G, Houbraken J, Boekhout T, Crous PW, Robert V, Verkley GJM (2019) Large-scale generation and analysis of filamentous fungal DNA barcodes boosts coverage for kingdom fungi and reveals thresholds for fungal species and higher taxon delimitation. *Studies in Mycology* 92(1): 135–154. <https://doi.org/10.1016/j.sismyco.2018.05.001>

- Wang M, Carver JJ, Phelan VV, Sanchez LM, Garg N, Peng Y, Nguyen DD, Watrous J, Kapono CA, Luzzatto-Knaan T, Porto C, Bouslimani A, Melnik AV, Meehan MJ, Liu WT, Crüsemann M, Boudreau PD, Esquenazi E, Sandoval-Calderón M, Kersten RD, Pace LA, Quinn RA, Duncan KR, Hsu CC, Floros DJ, Gavilan RG, Kleigrewe K, Northen T, Dutton RJ, Parrot D, Carlson EE, Aigle B, Michelsen CF, Jelsbak L, Sohlenkamp C, Pevzner P, Edlund A, McLean J, Piel J, Murphy BT, Gerwick L, Liaw CC, Yang YL, Humpf HU, Maansson M, Keyzers RA, Sims AC, Johnson AR, Sidebottom AM, Sedio BE, Klitgaard A, Larson CB, Boya CAP, Torres-Mendoza D, Gonzalez DJ, Silva DB, Marques LM, Demarque DP, Pociute E, O'Neill EC, Briand E, Helfrich EJN, Granatosky EA, Glukhov E, Ryffel F, Houson H, Mohimani H, Kharbush JJ, Zeng Y, Vorholt JA, Kurita KL, Charusanti P, McPhail KL, Nielsen KF, Vuong L, Elfeki M, Traxler MF, Engene N, Koyama N, Vining OB, Baric R, Silva RR, Mascuch SJ, Tomasi S, Jenkins S, Macherla V, Hoffman T, Agarwal V, Williams PG, Dai J, Neupane R, Gurr J, Rodríguez AMC, Lamsa A, Zhang C, Dorrestein K, Duggan BM, Almaliti J, Allard PM, Phapale P, Nothias LF, Alexandrov T, Litaudon M, Wolfender JL, Kyle JE, Metz TO, Peryea T, Nguyen DT, VanLeer D, Shinn P, Jadhav A, Müller R, Waters KM, Shi W, Liu X, Zhang L, Knight R, Jensen PR, Palsson B, Pogliano K, Linington RG, Gutiérrez M, Lopes NP, Gerwick WH, Moore BS, Dorrestein PC, Bandeira N (2016) Sharing and community curation of mass spectrometry data with Global Natural Products Social Molecular Networking. *Nature Biotechnology* 34(8): 828–837. <https://doi.org/10.1038/nbt.3597>
- Wang F, Liigand J, Tian S, Arndt D, Greiner R, Wishart DS (2021) CFM-ID 4.0: More Accurate ESI-MS/MS Spectral Prediction and Compound Identification. *Analytical Chemistry* 93(34): 11692–11700. <https://doi.org/10.1021/acs.analchem.1c01465>
- Wendt L, Sir EB, Kuhnert E, Heitkämper S, Lambert C, Hladki AI, Romero AI, Luangsa-ard JJ, Srikitkulchai P, Peršoh D, Stadler M (2018) Resurrection and emendation of the Hypoxylaceae, recognised from a multigene phylogeny of the Xylariales. *Mycological Progress* 17(1–2): 115–154. <https://doi.org/10.1007/s11557-017-1311-3>
- White TJ, Bruns TD, Lee S, Taylor JW (1990) Amplification and direct sequencing of fungal ribosomal RNA for phylogenetics. In: Innis MA, et al. (Eds) PCR protocols: a guide to methods and applications. Academic Press, San Diego, 315–322. <https://doi.org/10.1016/B978-0-12-372180-8.50042-1>
- Wibberg D, Stadler M, Lambert C, Bunk B, Spröer C, Rückert C, Kalinowski J, Cox RJ, Kuhnert E (2021) High quality genome sequences of thirteen Hypoxylaceae (Ascomycota) strengthen the phylogenetic family backbone and enable the discovery of new taxa. *Fungal Diversity* 106(1): 7–28. <https://doi.org/10.1007/s13225-020-00447-5>
- Zhang N, Castlebury LA, Miller AN, Huhndorf SM, Schoch CL, Seifert KA, Rossman AY, Rogers JD, Kohlmeyer J, Volkmann-Kohlmeyer B, Sung G-H (2006) An overview of the systematics of the Sordariomycetes based on a four-gene phylogeny. *Mycologia* 98(6): 1076–1087. <https://doi.org/10.1080/15572536.2006.11832635>
- Zhang D, Gao F, Jakovlić I, Zou H, Zhang J, Li WX, Wang GT (2020) PhyloSuite: An integrated and scalable desktop platform for streamlined molecular sequence data management and evolutionary phylogenetics studies. *Molecular Ecology Resources* 20(1): 348–355. <https://doi.org/10.1111/1755-0998.13096>

Supplementary material I

Supplementary information

Authors: Marjorie Cedeño-Sánchez, Esteban Charria-Girón, Christopher Lambert, J. Jennifer Luangsa-ard, Cony Decock, Raimo Franke, Mark Brönstrup, Marc Stadler

Data type: Alignments and MS raw data (PDF file)

Copyright notice: This dataset is made available under the Open Database License (<http://opendatacommons.org/licenses/odbl/1.0/>). The Open Database License (ODbL) is a license agreement intended to allow users to freely share, modify, and use this Dataset while maintaining this same freedom for others, provided that the original source and author(s) are credited.

Link: <https://doi.org/10.3897/mycokeys.95.98125.suppl1>